

RESEARCH ARTICLE

The oncogenic transcription factor FOXQ1 is a differential regulator of Wnt target genes

Giulia Pizzolato^{1,2}, Lavanya Moparathi^{1,2}, Simon Söderholm^{1,2}, Claudio Cantù^{1,2} and Stefan Koch^{1,2,*}

ABSTRACT

The forkhead box transcription factor FOXQ1 contributes to the pathogenesis of carcinomas. In colorectal cancers, FOXQ1 promotes tumour metastasis by inducing epithelial-to-mesenchymal transition (EMT) of cancer cells. FOXQ1 may exacerbate cancer by activating the oncogenic Wnt/ β -catenin signalling pathway. However, the role of FOXQ1 in the Wnt pathway remains to be resolved. Here, we report that FOXQ1 is an activator of Wnt-induced transcription and regulator of β -catenin target gene expression. Upon Wnt pathway activation, FOXQ1 synergises with the β -catenin nuclear complex to boost the expression of major Wnt targets. In parallel, we find that FOXQ1 controls the differential expression of various Wnt target genes in a β -catenin-independent manner. Using RNA sequencing of colorectal cancer cell lines, we show that Wnt signalling and FOXQ1 converge on a transcriptional programme linked to EMT and cell migration. Additionally, we demonstrate that FOXQ1 occupies Wnt-responsive elements in β -catenin target gene promoters and recruits a similar set of co-factors to the β -catenin-associated transcription factor Tcf711. Taken together, our results indicate a multifaceted role of FOXQ1 in Wnt/ β -catenin signalling, which may drive the metastasis of colorectal cancers.

KEY WORDS: Colorectal cancer, Forkhead box, Gene expression, Proteomics, Wnt signalling

INTRODUCTION

The Wnt/ β -catenin pathway is a major signalling cascade in development, tissue homeostasis and stem cell maintenance (Clevers, 2006; MacDonald et al., 2009). Wnt pathway dysregulation frequently occurs in major diseases, notably cancer, in which activating pathway mutations aberrantly stabilise the transcription co-factor β -catenin (Nusse and Clevers, 2017). This allows β -catenin to enter the nucleus and activate T-cell factor/lymphoid enhancer-binding factor (TCF/LEF) family transcription factors, which drive a transcriptional programme required for cell cycle progression and tissue self-renewal. Mounting evidence supports that the outcome of Wnt pathway activation is determined by numerous transcriptional co-regulators, which are recruited to

discrete target genes in a tissue- and context-specific manner (Masuda and Ishitani, 2017; Söderholm and Cantù, 2020).

Forkhead box (FOX) transcription factors have emerged as one such family of Wnt pathway regulators (Koch, 2021; Wang et al., 2015; Zhang et al., 2011; Zheng et al., 2019). Numerous FOX transcription factors act as activators or inhibitors of Wnt signalling, but the function of most FOX proteins in the Wnt pathway is incompletely understood (reviewed by Koch, 2021). Among these is FOXQ1, a putative oncogene in several types of carcinomas (Bagati et al., 2017; Kaneda et al., 2010; Qiao et al., 2011). In colorectal cancers (CRCs), FOXQ1 is one of the most highly upregulated genes, and has been linked to tumour growth and metastasis (Christensen et al., 2013; Kaneda et al., 2010). FOXQ1 has been identified as a candidate Wnt pathway activator in non-cancer and CRC cells (Moparathi et al., 2019; Peng et al., 2015), and has been shown to interact with β -catenin and TCF/LEF-associated transducin-like enhancer (TLE) proteins (Bagati et al., 2017). It has been suggested that FOXQ1 activates Wnt signalling by promoting the nuclear translocation of β -catenin (Peng et al., 2015; Xiang et al., 2020; Yang et al., 2022), or via the induction of canonical Wnt ligands (Kaneda et al., 2010; Xiang et al., 2020). However, the mode of action of FOXQ1 in Wnt signalling remains poorly defined.

Here, we identify FOXQ1 as a differential regulator of Wnt target gene expression. We find that FOXQ1 increases TCF/LEF activity to boost the transcription of specific Wnt targets. Additionally, we demonstrate that FOXQ1 controls the transcription of various target genes in a β -catenin/TCF-independent manner, which is determined by separate functional domains in its N and C termini. Finally, we show that FOXQ1 and Wnt signalling converge on a transcriptional programme involved in epithelial-to-mesenchymal transition (EMT) in CRC cells. Our findings suggest that FOXQ1 is a multifaceted regulator of Wnt/ β -catenin signalling, the induction of which in CRC may shift Wnt signalling from stem cell homeostasis and proliferation to EMT and metastasis.


RESULTS

FOXQ1 acts as differential regulator of Wnt/ β -catenin signalling

FOXQ1 has been identified as a candidate activator of Wnt/ β -catenin signalling (Moparathi et al., 2019; Peng et al., 2015). We first confirmed these findings using a β -catenin/TCF luciferase reporter (TOPflash; Veeman et al., 2003) in non-cancer 293T, and in HCT116, SW48 and DLD-1 CRC cells (Fig. 1A,B). In agreement with our earlier observations (Moparathi et al., 2019), exogenous Flag-tagged FOXQ1 activated the Wnt reporter, and strongly synergised with Wnt3a in TOPflash activation (Fig. 1A). In addition, FOXQ1 activated the TOPflash reporter in CRC cells with constitutive Wnt pathway activation (Fig. 1B). To determine whether physiological levels of FOXQ1 activate Wnt signalling, we next modulated FOXQ1 expression by CRISPR activation/

¹Wallenberg Centre for Molecular Medicine (WCMM), Linköping University, Linköping 58185, Sweden. ²Department of Biomedical and Clinical Sciences (BKV), Linköping University, Linköping 58185, Sweden.

*Author for correspondence (stefan.koch@liu.se)

 G.P., 0000-0002-0776-456X; L.M., 0000-0002-6030-3084; S.K., 0000-0003-3579-4229

This is an Open Access article distributed under the terms of the Creative Commons Attribution License (<https://creativecommons.org/licenses/by/4.0>), which permits unrestricted use, distribution and reproduction in any medium provided that the original work is properly attributed.

Handling Editor: John Heath

Received 1 April 2022; Accepted 7 September 2022

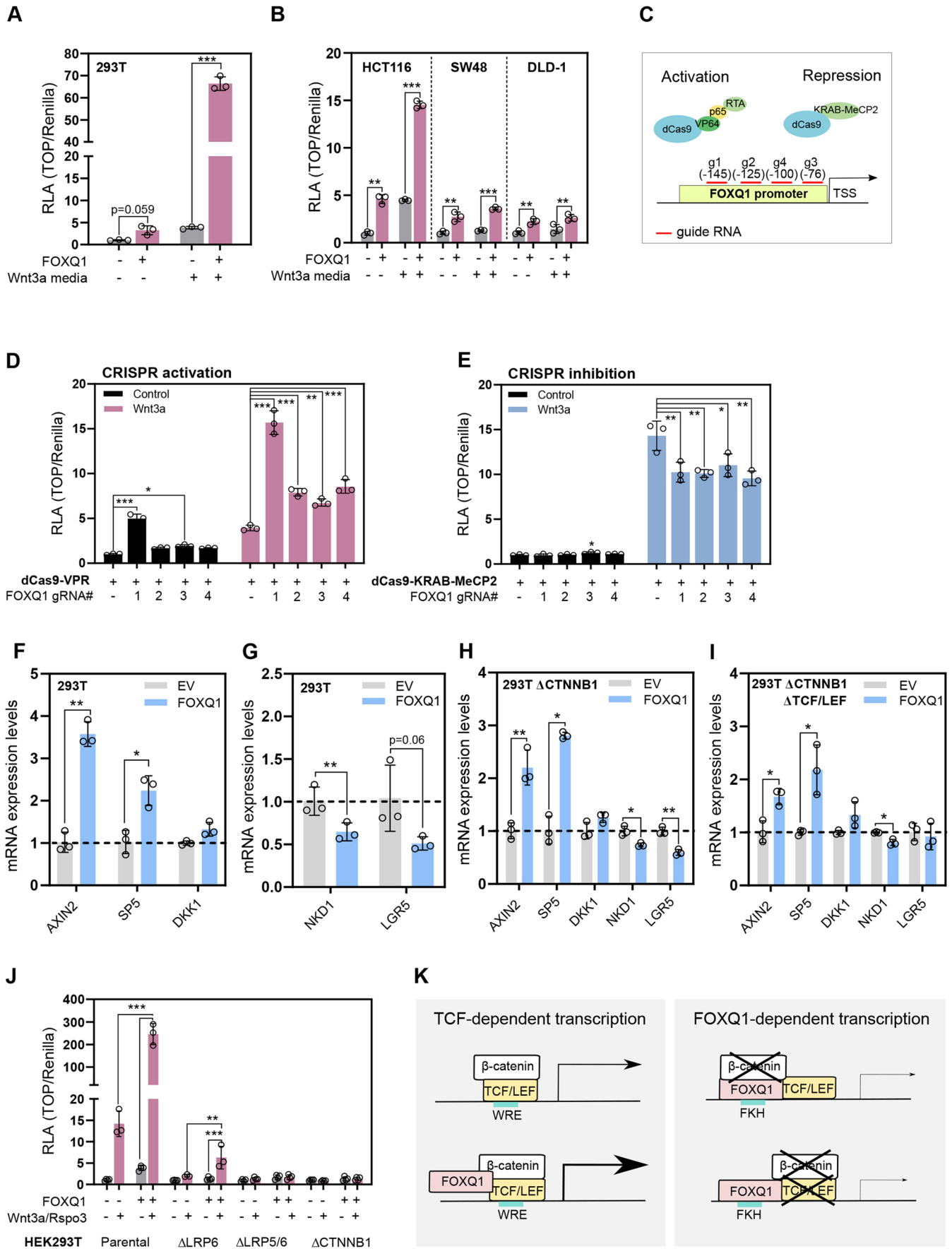


Fig. 1. See next page for legend.

Fig. 1. FOXQ1 is a differential regulator of Wnt/ β -catenin signalling. (A,B) FOXQ1 activates the β -catenin/TCF luciferase reporter TOPflash (TOP, normalised to Renilla control) in 293T cells, particularly in the presence of Wnt3a-conditioned media (CM). FOXQ1 also activates the TOPflash reporter in HCT116, SW48 and DLD-1 cells, which display constitutive Wnt pathway activity. Data are normalised to the untreated empty vector control for each cell line, and show one representative of $n=3$ independent experiments with biological triplicates. RLA, relative luciferase activity. (C) Schematic representation of the CRISPR-mediated FOXQ1 transcriptional activation or inhibition (CRISPRa/i). dCas9-VPR or dCas9-KRAB-MeCP2 constructs were targeted to the FOXQ1 promoter using four non-overlapping guide RNAs (g1-4). Distance of gRNAs from the transcription start site (TSS) is indicated in parentheses. (D) TOPflash reporter assay in 293T cells upon CRISPR activation of FOXQ1. Where indicated, cells were treated with Wnt3a-conditioned media. FOXQ1 induction by g1 and g3 significantly activated Wnt/ β -catenin signalling in untreated cells. All gRNAs led to Wnt signalling activation in Wnt3a-treated cells. Data show one representative of $n=3$ independent experiments with biological triplicates. (E) TOPflash reporter assay in 293T upon CRISPR inhibition of FOXQ1. FOXQ1 repression by g1-4 significantly reduced TOPflash activity after Wnt3a stimulation. Data show results from one experiment with biological triplicates. (F,G) qPCR analysis of Wnt target gene expression in 293T cells. FOXQ1 induced *AXIN2*, *SP5* and *DKK1* expression. In contrast, FOXQ1 repressed *NKD1* and *LGR5*. (H,I) qPCR analysis of Wnt target genes in 293T Δ CTNNB1 (H) and penta-KO (I) cells. FOXQ1 induced *AXIN2* and *SP5*, and repressed *NKD1* and *LGR5* in the absence of β -catenin and TCF/LEF proteins, albeit to a lesser extent to the repression in parental cells. (J) Epistasis assays in normal and gene-edited 293T cells. Where indicated, cells were treated with Wnt3a and R-spondin 3 Δ C (Rspo3)-conditioned media. Loss of the Wnt co-receptor LRP6 attenuated FOXQ1-dependent TOPflash reporter activation. Loss of LRP5/6 or β -catenin (CTNNB1) blocked reporter activation by FOXQ1. The graph shows one representative of $n=2$ independent experiments with biological triplicates. (K) Schematic model of the dual functions of FOXQ1 in the Wnt pathway: (1) FOXQ1 enhances TCF-mediated transcriptional responses (left); (2) FOXQ1 regulates the transcription of Wnt target genes independently of β -catenin and TCF/LEF (right). Data are displayed as mean \pm s.d. For qPCR experiments, samples were collected after 24 h, and individual data points from biological triplicates are displayed. Statistical significance was determined by Welch's *t*-test (A,B,F-I), or ANOVA with Dunnett's (D,E) or Tukey's (J) post-hoc tests (* $P<0.05$, ** $P<0.01$, *** $P<0.001$).

inhibition (Chavez et al., 2015; Yeo et al., 2018). CRISPR activation using four non-overlapping guide RNAs (gRNA) targeting the FOXQ1 promoter increased FOXQ1 levels in 293T cells up to 20-fold (Fig. 1C; Fig. S1A-C), which is a change in expression comparable with that observed in CRC (Christensen et al., 2013). We found that CRISPR activation of FOXQ1 significantly increased TOPflash activity in 293T and HCT116 cells, especially in synergy with Wnt3a (Fig. 1D; Fig. S1D). Conversely, CRISPR inhibition reduced Wnt reporter activity in Wnt3a-treated 293T (Fig. 1E) and Caco-2 (Fig. S1E) cells, suggesting Wnt pathway regulation at physiologically relevant FOXQ1 levels.

To determine whether Wnt reporter activation by FOXQ1 is reflected in a corresponding transcriptional response, we next tested the regulation of several well-characterised Wnt target genes by qPCR in 293T cells. Consistent with the TOPflash data, we observed that FOXQ1 increased the expression of *AXIN2*, *SP5* and *DKK1* (Fig. 1F). However, other targets, such as *NKD1* and *LGR5*, were instead repressed by FOXQ1 (Fig. 1G), arguing against a general activation of the canonical Wnt pathway. We therefore repeated these experiments in 293T cells with genetic deletion of either β -catenin only (Δ CTNNB1) or β -catenin and all four TCF/LEF family transcription factors (penta-KO; Doumpas et al., 2019). Although the effect was smaller in penta-KO cells, FOXQ1

differentially regulated Wnt target genes to a similar degree across all cell lines (Fig. 1H,I). In contrast, FOXQ1 was unable to promote TOPflash activity in cells lacking β -catenin or the Wnt co-receptors LRP5/6 (Fig. 1J). We conclude that FOXQ1 enhances TCF/LEF reporter activity, and that it additionally acts independently of β -catenin and TCF/LEF factors to regulate the transcription of Wnt target genes (Fig. 1K).

FOXQ1 boosts TCF/LEF-dependent transcription at the level of the Wnt transcriptional complex

The aforementioned observations suggested that FOXQ1 has separate modes of action in the activation of TCF/LEF-dependent transcription and the regulation of Wnt target genes. We first investigated how FOXQ1 promotes Wnt reporter activity, which may be explained by the FOXQ1-dependent induction of Wnt ligands (Kaneda et al., 2010; Xiang et al., 2020). Indeed, TOPflash activation by FOXQ1 was blocked by the porcupine inhibitor LGK974, which prevents the secretion of Wnt ligands (Fig. 2A,B). This was particularly evident after Wnt receptor stabilisation by R-spondin 3, whereas LGK974 had no effect in the presence of exogenous Wnt3a. Moreover, LGK974 was less potent in HCT116 cells with constitutively stabilised β -catenin (Fig. S2A). qPCR of all Wnt ligands in 293T cells showed that FOXQ1 significantly altered the expression of several Wnt ligands, albeit to a lesser extent compared with the similarly potent Wnt activator FOXB2 (Fig. 2C; Fig. S2B), which we previously identified as a major activator of Wnt ligand expression (Moparthi et al., 2019). To unambiguously determine whether TOPflash activation by FOXQ1 can be explained by Wnt ligand induction, we uncoupled Wnt ligand binding from Wnt receptor activation by re-expressing constitutively active LRP6 (LRP6 Δ E1-4; Davidson et al., 2005) in 293T Δ LRP5/6 cells (Fig. 2A,D). FOXQ1, but not FOXB2, synergised with LRP6 Δ E1-4 in TOPflash activation (Fig. 2D). Moreover, FOXQ1 activated the Wnt reporter when β -catenin was artificially stabilised by the GSK3 inhibitor CHIR99021 (Fig. 2E; Fig. S2C). Conversely, reducing β -catenin levels with the tankyrase inhibitor XAV939 significantly reduced the activation of Wnt signalling by FOXQ1 (Fig. 2F; Fig. S2D). Additionally, FOXQ1 strongly synergised with exogenous wild-type or constitutively active (S33Y) β -catenin in TOPflash activation in 293T Δ CTNNB1 cells (Fig. S2E). Interestingly, we observed that FOXQ1 also synergised with a constitutively active LEF1 Δ N-VP16 deletion construct lacking its β -catenin-binding domain in TOPflash activation in 293T cells (Aoki et al., 1999) (Fig. 2G). Consistent with reporter activation, FOXQ1 increased *AXIN2* expression in synergy with the LEF1 deletion construct in 293T parental and penta-KO cells (Fig. 2H). Taken together, these results suggest that FOXQ1 enhances TCF/LEF signalling at the level of the Wnt transcriptional complex, and that this function is independent of its ability to induce Wnt ligands.

Wnt reporter activation by FOXQ1 does not require association with β -catenin and TCF

FOXQ1 directly interacts with β -catenin (Bagati et al., 2017), and may thus control Wnt pathway activation through association with the Wnt transcriptional complex. We first confirmed this earlier finding by co-immunoprecipitation (co-IP) assays in nuclear extracts of 293T cells. Indeed, pull-down of FOXQ1 precipitated endogenous β -catenin (Fig. 3A). Additionally, we found that FOXQ1 associated with TCF7L2 and LEF1, and this interaction did not require β -catenin (Fig. 3B,C). Finally, similar to other FOX proteins (Zhang et al., 2011; Zheng et al., 2019), exogenous FOXQ1

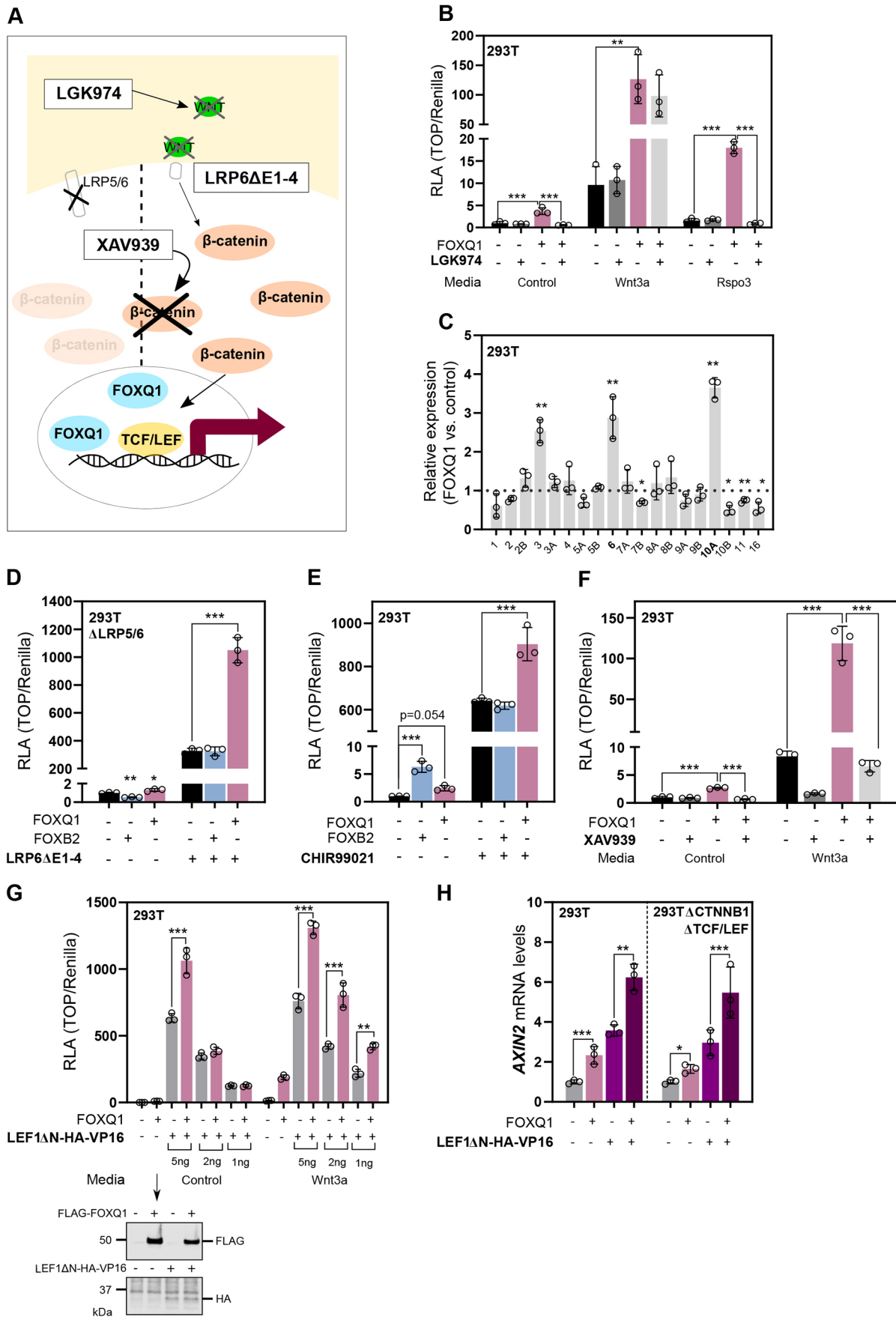


Fig. 2. See next page for legend.

Fig. 2. FOXQ1 promotes TCF/LEF signalling at the level of the Wnt transcriptional complex.

(A) Schematic showing the mode of action of the porcupine inhibitor LGK974, the constitutively active LRP6 Δ E1-4 construct and the tankyrase inhibitor XAV939. (B) TOPflash assay in 293T cells in the presence of LGK974. Treatment with LGK974 (10 nM) attenuated FOXQ1-dependent Wnt activation, especially in the presence of exogenous Rspo3. Data show one representative experiment of $n=3$ independent experiments with biological triplicates. (C) qPCR analysis of all 19 Wnt ligands in 293T cells. FOXQ1 significantly altered the expression of several Wnt genes, particularly *WNT3*, *WNT6* and *WNT10A*. Samples were collected after 24 h, and data are displayed as fold change compared with empty vector control from biological triplicates. (D) TOPflash assay in 293T Δ LRP5/6 cells. Where indicated, cells were transfected with a constitutively active LRP6 construct lacking the extracellular ligand binding domains (LRP6 Δ E1-4). FOXQ1, but not FOXB2, strongly activated the TOPflash reporter in the presence of LRP6 Δ E1-4. Data show one representative of $n=3$ independent experiments with biological triplicates. (E) TOPflash assay in wild-type 293T cells. Where indicated, cells were treated with GSK3 inhibitor CHIR99021 (5 μ M). FOXQ1, but not FOXB2, significantly activated the reporter construct in synergy with CHIR99021. Data show one representative of $n=3$ independent experiments with biological triplicates. (F) TOPflash assay in 293T cells. Where indicated, cells were treated with Wnt3a conditioned media and XAV939 (5 μ M). FOXQ1-dependent Wnt activity was significantly reduced upon β -catenin de-stabilization by XAV939. Data show one representative of $n=3$ independent experiments with biological triplicates. (G) TOPflash assay in 293T cells. Where indicated, cells were transfected with a constitutive active LEF1 Δ N-VP16 construct at decreasing concentrations. FOXQ1 synergised with the LEF1 Δ N-VP16 construct in reporter activation. Cell lysates from the assay were used for immunoblot to confirm protein expression. Data show one representative of $n=3$ independent experiments with biological triplicates. (H) qPCR analysis of *AXIN2* expression in 293T parental and penta-KO cells in the presence of the LEF1 Δ N-VP16 construct. Samples were collected after 24 h, and individual data points from biological triplicates are displayed. FOXQ1 significantly increased *AXIN2* expression in synergy with LEF1 Δ N-VP16 construct in both cell lines. Data are displayed as mean \pm s.d. Statistical significance was determined by ANOVA with Tukey's (B,F,G,H) or Dunnett's (D,E) post-hoc test, or Welch's *t*-test (C) (* $P<0.05$, ** $P<0.01$, *** $P<0.001$).

increased the association of β -catenin with TCF7L2 and LEF1 (Fig. S3A,B). To determine the FOXQ1 protein domains required for its interaction with the Wnt transcriptional complex, we generated FOXQ1 deletion constructs lacking the entire N or C terminus (FOXQ1 Δ N and Δ C, respectively) (Fig. 3D). First, we tested these FOXQ1 constructs in TOPflash reporter assays. Whereas FOXQ1 Δ N exhibited dramatically reduced reporter activation in 293T and HCT116 cells, FOXQ1 Δ C essentially phenocopied the full-length protein, except in Wnt3a-treated 293T cells where its activity was reduced (Fig. 3E,F). We then repeated our earlier co-IP experiments using these constructs. Surprisingly, FOXQ1 Δ C was unable to interact with β -catenin and TCF7L2 (Fig. 3G,H), despite its activity in TOPflash assays. We conclude that FOXQ1 directly engages the Wnt transcriptional complex via its C terminus, but that this interaction is largely dispensable for Wnt reporter activation, which instead requires the FOXQ1 N-terminus (Fig. 3I).

FOXQ1 N and C termini differentially regulate the transcription of Wnt target genes

We next investigated the effect of the FOXQ1 deletion constructs on Wnt target gene expression. FOXQ1 Δ N was unable to induce any tested gene that was activated by the full-length protein (*AXIN2*, *SP5* and *DKK1*; Fig. 4A) and did not synergise with Wnt3a, but fully repressed negatively regulated genes (*NK1* and *LGR5*; Fig. 4B). In contrast, FOXQ1 Δ C induced positively regulated genes to a similar or greater extent compared with full-length FOXQ1 (Fig. 4A), albeit with reduced Wnt responsiveness, but was unable to repress *NK1*

and *LGR5* (Fig. 4B). Finally, only full-length FOXQ1 induced *LEF1* expression, which required Wnt3a stimulation (Fig. 4B). Because our results suggested that the FOXQ1 C terminus mainly mediates repression of FOXQ1 target genes, we additionally tested the deletion constructs using the forkhead box reporter 10x UFR-luc, which is strongly negatively regulated by full-length FOXQ1 (Moparthi and Koch, 2020). Consistent with our earlier findings, loss of the FOXQ1 C terminus significantly de-repressed the forkhead box reporter, whereas deletion of the N terminus had no effect in this assay (Fig. 4C). It has been suggested that differential functions of FOXQ1 can be explained by recruitment of β -catenin, which displaces TLE proteins and thereby de-represses FOXQ1 target genes in carcinoma cells (Bagati et al., 2017). However, re-expression of β -catenin in 293T Δ CTNBN1 or penta-KO cells had no effect on the regulation of forkhead box reporter activity by any of the FOXQ1 constructs (Fig. 4D,E).

Finally, to further investigate whether the altered transcriptional activity of the FOXQ1 deletion constructs affects cell proliferation, we performed an MTT assay using 293T and HCT116 cells (Fig. 4F). FOXQ1 and both FOXQ1 truncation constructs significantly increased the proliferation of HCT116 CRC cells. In contrast, FOXQ1 and FOXQ1 Δ N in particular decreased the proliferation of 293T cells (Fig. 4F). Collectively, these observations suggest that the FOXQ1 N and C terminus have discrete functions in the induction and repression of Wnt target genes, respectively, which coincides with different signalling and functional outcomes in non-cancer and CRC cell lines (Fig. 4G).

FOXQ1 occupies Wnt-responsive elements at Wnt target genes and shares multiple transcription co-factors with TCF/LEF

Our experiments in β -catenin-deficient cells indicated that FOXQ1 controls selected Wnt target genes independently of the Wnt transcriptional complex. We therefore investigated whether FOXQ1 occupies known Wnt-responsive elements (WRE) in β -catenin/TCF target genes. Bioinformatics analyses highlighted numerous putative FOXQ1-binding sites at or close to WREs (Fig. S4A). In addition, we used public chromatin immunoprecipitation (ChIP)-seq datasets of other FOX family members with highly similar DNA-binding motifs (Fig. S4B-D) as a proxy for FOXQ1, and identified several WREs that are co-occupied by FOXs and β -catenin/Tcf7l1 (Fig. 5A; Fig. S4E,F). To test whether FOXQ1 physically occupies these WREs, we then performed ChIP followed by qPCR in 293T cells, and observed FOXQ1 signal enrichment specifically at the WRE located within the *AXIN2* promoter (Zimmerli et al., 2020), whereas no enrichment was seen at adjacent chromosomal regions (Fig. 5B).

Because these results suggest that FOXQ1 is capable of binding at selected Wnt target genes, we then probed the FOXQ1 interactome by proximity proteomics (Branon et al., 2018; Cho et al., 2020) in 293T cells using a N-terminal TurboID-FOXQ1 fusion construct, which retained activity in TOPflash assays (Fig. S5A,B). Mass spectrometry analysis following streptavidin pull-down of biotinylated proteins identified nearly 400 candidate interactors that were significantly enriched compared with control. Gene ontology analysis of these hits revealed that FOXQ1 proximal proteins are primarily involved in mRNA processing, chromatin remodelling and transcription regulation, but notably also β -catenin/TCF complex assembly (Fig. S5C, Table S1). To identify common interactors of FOXQ1 and the Wnt transcriptional complex, we compared the proteomics results with a published BioID

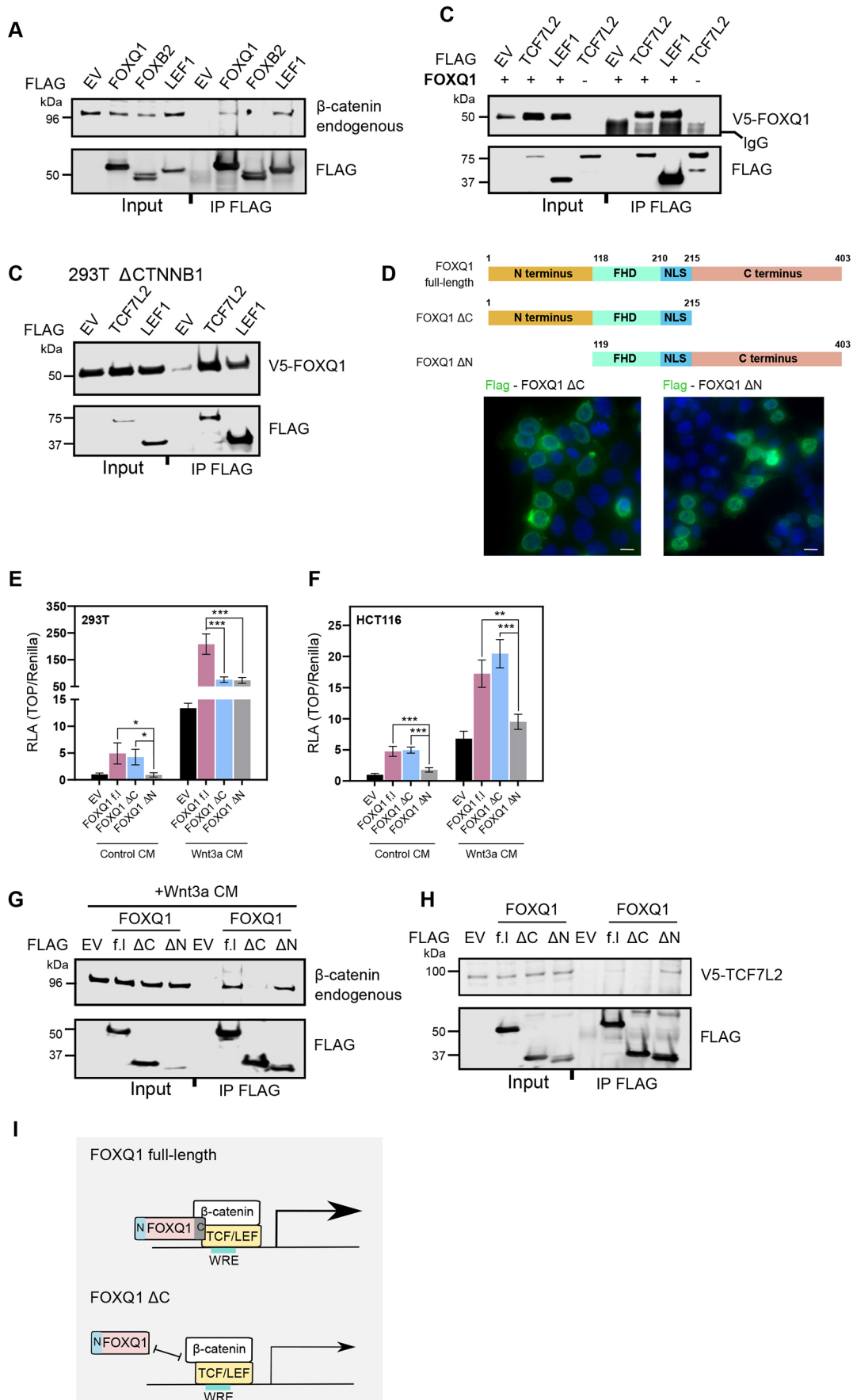


Fig. 3. See next page for legend.

Fig. 3. FOXQ1/ β -catenin/TCF/LEF interactions are dispensable for Wnt activation. (A) Co-immunoprecipitation assay in nuclear lysates of 293T cells. Overexpressed Flag-tagged proteins were pulled down using a Flag antibody, and endogenous β -catenin was detected by immunoblotting. FOXB2 and LEF1 were used as negative and positive controls, respectively. Data show results from one experiment. (B) Co-immunoprecipitation from nuclear lysates of 293T cells. Following pull-down of Flag-tagged TCF7L2 and LEF1, V5-FOXQ1 was detected by immunoblotting. Data show results from one experiment. (C) Co-immunoprecipitation from nuclear lysates of 293T Δ CTNNB1 cells. Flag-tagged TCF7L2 and LEF1 proteins were pulled down in the presence of V5-FOXQ1. Immunoblot detection revealed TCF7L2/LEF1 interaction with FOXQ1 in the absence of β -catenin. A representative blot from $n=2$ independent experiments is shown. (D) Top: schematic representation of Flag-FOXQ1 deletion constructs used in subsequent assays. Numbers indicate amino acid positions. FHD, (DNA-binding) forkhead domain; NLS, nuclear localisation sequence. Bottom: representative immunofluorescence microscopy images showing nuclear localization of Flag-tagged FOXQ1 deletion constructs (green, with nuclei counterstained in blue) in colorectal cancer HCT116 cells. Images are representative of $n=2$ independent experiments. Scale bars: 20 μ m. (E) TOPflash assay in 293T cells. The FOXQ1 C terminus was found to be dispensable for Wnt pathway activation in untreated (i.e. low Wnt) cells. In high Wnt conditions, neither construct activated TOPflash to the same extent as full-length (f.l) FOXQ1. Data show one representative of $n=3$ independent experiments with biological triplicates. (F) TOPflash assay in HCT116 cells. The FOXQ1 Δ C construct activated Wnt signalling to the same extent as full-length FOXQ1. Data show one representative of $n=3$ independent experiments with biological triplicates. (G) Co-immunoprecipitation assay in nuclear lysates of 293T cells treated with Wnt3a conditioned media. Following Flag pull-down of FOXQ1 constructs, endogenous β -catenin was detected by immunoblotting. FOXQ1 Δ C was unable to bind β -catenin to any substantial degree. Representative blot from $n=2$ independent experiments. (H) Co-immunoprecipitation assay in nuclear lysates of 293T cells. Flag-tagged FOXQ1 constructs were pulled down in the presence of V5-TCF7L2. FOXQ1 Δ C was unable to bind TCF7L2 to any substantial degree. Data show results from one experiment. (I) Schematic representation of the main conclusions from the FOXQ1 deletion constructs. FOXQ1 engages the Wnt transcriptional complex via its C terminus, but this interaction is dispensable for Wnt reporter activation, which instead requires the FOXQ1 N terminus. Data are displayed as mean \pm s.d. Statistical significance was determined by Tukey's post-hoc test following ANOVA (E,F) (* $P<0.05$, ** $P<0.01$, *** $P<0.001$).

dataset of Tcf711 interactors in mouse embryonic stem cells (Moreira et al., 2018 preprint). As these data include cells treated with the Wnt pathway activator CHIR99021, we repeated our proteomics studies with CHIR-treated cells for better comparison. CHIR treatment notably changed the interactome of FOXQ1, with approximately one-third of the hits only being identified in the untreated or treated condition, suggesting dynamic rearrangement of the FOXQ1 transcriptional complex upon Wnt pathway activation (Fig. 5C). After stringent uniform data filtration and analysis (Fig. S5D), we observed that the majority of high-confidence FOXQ1 interactors were shared with Tcf711 (Fig. 5D–G; Tables S2 and S3). Besides TLE3 and TLE4 (Bagati et al., 2017), these included other known regulators of Wnt/ β -catenin signalling, such as the histone acetyltransferases CREBBP and EP300 (Li et al., 2007; Walker et al., 2015), the chromatin remodelling factor SMARCA4 (Barker et al., 2001) and the transcription activator CCAR1 (Ou et al., 2009). Finally, to validate some of these interactors, we performed co-immunoprecipitation assays in 293T cells, and confirmed that FOXQ1 precipitated endogenous TLEs and CREBBP (Fig. 5H,I). Silencing of CREBBP by RNA interference decreased FOXQ1-induced TOPflash activation in 293T cells to a larger extent than the empty vector condition (Fig. 5J; Fig. S5E), thus identifying CREBBP as a potential functional interactor of FOXQ1 in the Wnt pathway. We conclude that FOXQ1 binds in the proximity of WREs

at specific Wnt target loci, and may recruit many of the same transcription co-factors as TCF/LEF to effect target gene expression independently of the Wnt transcriptional complex.

FOXQ1 alters the transcriptome of colorectal cancer cells

To place our findings in the context of general FOXQ1 biology, we performed bulk RNA sequencing of FOXQ1 or vector-transfected HCT116 cells with or without Wnt3a treatment (Fig. S6A). FOXQ1 overexpression significantly altered the expression of thousands of protein-coding genes, with an even split between induced and repressed genes (Fig. 6A; Fig. S6B). Gene ontology analysis of differentially expressed genes indicated that genes induced by FOXQ1 are involved in cell proliferation and differentiation, extracellular matrix organisation, and cell migration, consistent with its known function in tumour metastasis. Conversely, genes repressed by FOXQ1 were found to be involved in RNA processing and post-transcriptional modification (Fig. S6C,D). We additionally performed gene set enrichment analysis (GSEA; Subramanian et al., 2005) against all hallmark gene sets curated in the Molecular Signatures Database (Liberzon et al., 2015), discarding results with an adjusted $P>0.05$. GSEA indicated that FOXQ1 overexpression induced genes downregulated by KRAS activation and suppressed MYC target genes (Fig. S6E), collectively suggesting that inhibition of KRAS and MYC signalling are major functions of FOXQ1 in CRC cells.

With regard to Wnt signalling, we found that Wnt3a treatment significantly changed the expression of 166 genes in HCT116 cells (Fig. S6B). Using this gene list as input for GSEA, we observed an apparent but non-significant enrichment upon FOXQ1 overexpression, which was the case both for genes induced and repressed by Wnt3a (Fig. 6B). We repeated this analysis using a manually curated list of genes induced by β -catenin in CRC cells (Herbst et al., 2014), with essentially identical results (Fig. S6F). Additionally, we re-analysed a published microarray dataset of DLD-1 CRC cells with shRNA-mediated depletion of FOXQ1 (Tang et al., 2020). GSEA of the 166 Wnt-regulated genes (see above) showed that loss of FOXQ1 was associated with reduced expression of Wnt-induced genes (Fig. S6G).

Comparing Wnt3a-treated cells with or without exogenous FOXQ1, we found that FOXQ1 significantly altered the expression of most Wnt target genes. Besides well-characterised Wnt targets such as AXIN2 and NOTUM, we noted that FOXQ1 strongly boosted the expression of many cancer-associated genes such as *CHI3L1* and *CEMIP* (Fig. 6C), which have been implicated in epithelial-to-mesenchymal transition (EMT) and metastasis (Rodrigues et al., 2019; Zhao et al., 2020). Consistently, GSEA showed significant enrichment of the hallmark gene set for EMT in FOXQ1 plus Wnt3a cells (Fig. 6D), but not in FOXQ1 or Wnt3a only cells (adjusted P -values of 0.59 and 1, respectively).

Taken together, these transcriptomics analyses support that FOXQ1 differentially regulates the expression of Wnt target genes, and indicate that this is not a major function of FOXQ1 in CRC cells. However, the data additionally suggest that FOXQ1 and Wnt signalling converge on genes relevant for EMT, which may have important implications for cancer biology.

DISCUSSION

In this study, we identify the carcinoma oncogene FOXQ1 as a regulator of Wnt target gene expression. Earlier studies suggested that FOXQ1 activates Wnt/ β -catenin signalling (Moparthi et al., 2019; Peng et al., 2015), but its mode of action in the Wnt pathway remained poorly defined. We now report that FOXQ1 has at least two distinct functions: it controls the expression of major Wnt target

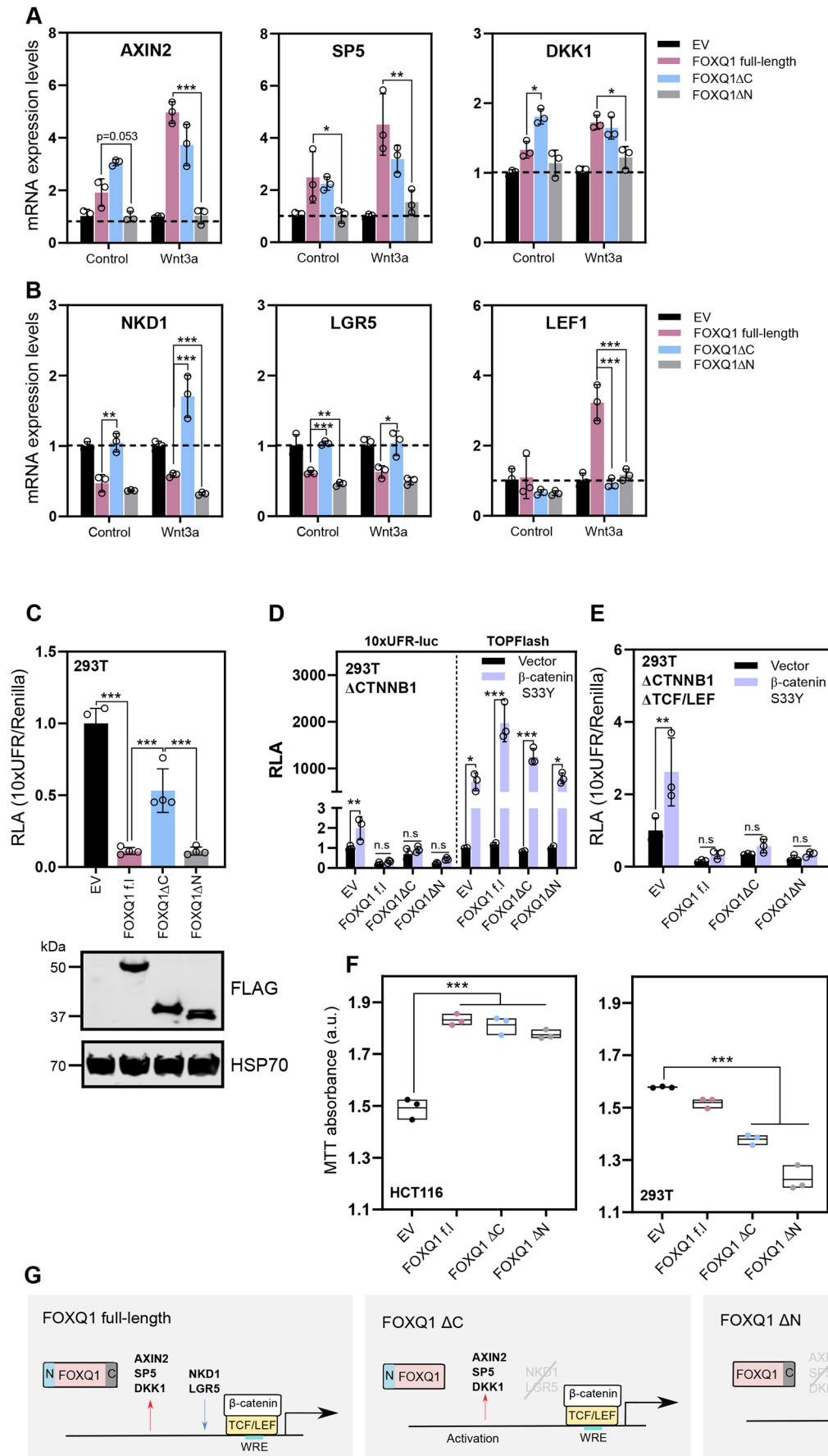


Fig. 4. See next page for legend.

Fig. 4. The FOXQ1 N and C termini differentially regulate Wnt signalling. (A,B) qPCR analysis of selected Wnt target genes upon expression of FOXQ1 constructs in 293T cells. (A) FOXQ1 Δ C, but not FOXQ1 Δ N, induced *AXIN2*, *SP5* and *DKK1*, similarly to full-length FOXQ1. (B) FOXQ1 Δ N, but not FOXQ1 Δ C, repressed *NKD1* and *LGR5* similarly to full-length FOXQ1. *LEF1* was induced exclusively by full-length FOXQ1 upon Wnt3a treatment. (C) FOXQ1 transcriptional activity determined with a forkhead box reporter plasmid (10x UFR-luc) in 293T cells. Loss of the FOXQ1 C terminus resulted in significantly weaker transcriptional repression compared with the other constructs. Cell lysates from the assay were used for immunoblot to confirm equal expression. Data show one representative of $n=2$ independent experiments with four biological replicates. (D) Luciferase assay using the 10x UFR-luc and TOPflash reporters in 293T Δ TNNB1 cells. FOXQ1 transcription repression at forkhead-binding sites was not rescued by re-expression of β -catenin S33Y, despite their synergy in the TOPflash reporter assay. Data show one representative of $n=3$ independent experiments with biological triplicates. (E) Luciferase assay using the 10x UFR-luc reporter in 293T penta-KO cells. β -Catenin did not affect FOXQ1 transcriptional activity at forkhead-binding sites in penta-knockout cells. Data show one representative of $n=3$ independent experiments with biological triplicates. (F) MTT assays in HCT116 and 293T cells. FOXQ1 significantly increased the proliferation of CRC HCT116 cells, as opposed to a decreased proliferation in the non-cancer 293T cell line. Boxes represent the minimum to maximum values, with the mean marked by a line. (G) Schematic representation of the different functions of FOXQ1 protein domains. The N and C terminus mediate transcriptional activation and repression of Wnt genes, respectively. Data are displayed as mean \pm s.d. Where indicated, cells were treated with Wnt3a-conditioned media. For qPCR experiments, samples were collected after 24 h, and individual data points from biological triplicates are displayed. Statistical significance was determined by Tukey's post-hoc test following ANOVA (A-F) (n.s. not significant; * $P<0.05$, ** $P<0.01$, *** $P<0.001$).

genes independently of β -catenin and TCF/LEF transcription factors; and it boosts the activity of TCF/LEF upon activation of the Wnt signalling pathway. Collectively, these results suggest that FOXQ1 regulates the Wnt transcriptional output to reinforce and specify the outcome of Wnt signalling in a context-dependent manner. Importantly, our data indicate that FOXQ1 may cooperate with Wnt signalling in promoting the transcription of genes involved with epithelial-to-mesenchymal transition (EMT) and migration of cancer cells.

Chronically elevated Wnt signalling due to activating pathway mutations is a hallmark feature of sporadic CRC. FOXQ1 has been identified as a direct transcriptional target of β -catenin and TCF (Christensen et al., 2013), and it is consistently one of the most highly induced genes in colorectal carcinomas (Christensen et al., 2013; Kaneda et al., 2010). Overexpression of FOXQ1 in CRC cells triggers EMT, tumour metastasis and resistance to chemotherapeutics (Abba et al., 2013; Kaneda et al., 2010; Liu et al., 2017; Peng et al., 2015). Accordingly, FOXQ1 expression is an independent prognostic marker for worse prognosis in individuals with CRC (Weng et al., 2016). It is unclear at this time whether FOXQ1 drives tumour progression in collaboration with or independently of β -catenin and TCF/LEF. Wnt pathway activation itself can cause EMT and treatment resistance in advanced CRC (Basu et al., 2016; Zhan et al., 2017), and, in fact, induction of the prototypical Wnt target *AXIN2* alone is sufficient to trigger EMT in CRC cell lines (Wu et al., 2012). Our results indicate that FOXQ1 preferentially boosts the expression of EMT-related Wnt target genes. Wnt-dependent induction of FOXQ1 may thus aid in committing cells to a Wnt response that is biased towards EMT and metastasis in cancer.

We observed that FOXQ1 controls the transcription of major Wnt target genes in the absence of β -catenin and TCF/LEF transcription factors. How FOXQ1 regulates gene transcription requires further

investigation, but the results from our proteomics and bioinformatics analyses suggest that FOXQ1 occupies some of the same genomic loci as TCF/LEF, and interacts with a similar set of transcription co-factors to potentially phenocopy TCF/LEF on specific target gene promoters. Consistent with this hypothesis, it has been suggested that EMT induction by FOXQ1 hinges on the regulation of N-cadherin (*CDH2*) in a manner remarkably similar to the regulation of Wnt-dependent transcription (Bagati et al., 2017). Bagati et al. reported that FOXQ1 suppresses *CDH2* by recruitment of TLE proteins, which also function as the main transcriptional repressors on TCF/LEF transcription factors (Daniels and Weis, 2005). In CRC cells, chronically high levels of β -catenin may displace TLEs from FOXQ1, thereby causing *CDH2* de-repression and ultimately EMT (Bagati et al., 2017). Indeed, we found that removal of the FOXQ1 C terminus, which contains a putative TLE-binding EH1 domain (Yaklichkin et al., 2007), de-repressed *NKD1* and *LGR5*. However, we did not observe an effect of β -catenin on general transcriptional repression by FOXQ1, suggesting that the interaction of β -catenin with FOXQ1 might have gene-specific functions.

On the other hand, we observed that FOXQ1 strongly potentiates the transcriptional activity of TCF/LEF in Wnt reporter assays even at saturating β -catenin levels, and synergises with Wnt3a in the activation of important Wnt target genes, including *AXIN2*. It is currently unclear how FOXQ1 boosts the activity of β -catenin and TCF/LEF. Earlier studies reported that FOXQ1 induces various Wnt agonists (Kaneda et al., 2010; Xiang et al., 2020), and increases the nuclear translocation of β -catenin (Peng et al., 2015; Yang et al., 2022). Moreover, FOXQ1 has been shown to physically interact with β -catenin and TLEs (Bagati et al., 2017), which raised the possibility that it may stabilise the Wnt transcriptional complex in a similar manner as, for example, FOXM1 and FOXG1 (Zhang et al., 2011; Zheng et al., 2019). We found that FOXQ1 significantly induced multiple Wnt ligands, but unlike the comparably strong Wnt activator FOXB2 (Moparthi et al., 2019), ligand induction was largely dispensable for its activity in reporter assays. Similarly, even though we found that FOXQ1 enhances the association of β -catenin with TCF/LEF, direct interaction of FOXQ1 with β -catenin/TCF was not required for increasing their transcriptional activity, at least in reporter assays. However, Wnt ligand induction and β -catenin binding may have additive effects on other functions of FOXQ1 in the Wnt pathway, which could explain the different activity of our FOXQ1 constructs in reporter assays in 293T and HCT116 cells. Moreover, FOXQ1 may recruit additional transcription co-factors such as CREBBP and EP300 to increase the transcriptional activity of β -catenin, similar to FOXF1 (Walker et al., 2015).

Finally, it has recently been suggested that FOXQ1 controls β -catenin subcellular shuttling indirectly via induction of SIRT1 (Yang et al., 2022), which also plays a prominent role in EMT and metastasis of various types of cancer, including CRC (Byles et al., 2012; Cheng et al., 2016). However, the contribution of SIRT1 to FOXQ1-dependent Wnt pathway regulation and tumour progression requires further investigation.

In summary, our study outlines a surprisingly multifaceted role of the carcinoma oncogene FOXQ1 in the regulation of Wnt/ β -catenin signalling. Considering the crosstalk between FOXQ1 and Wnt signalling in CRC and their significant contribution to promoting EMT and cancer metastasis, further exploration of the FOXQ1 transcriptome and interactome is clearly warranted to potentially uncover therapeutic vulnerabilities in Wnt-driven cancers.

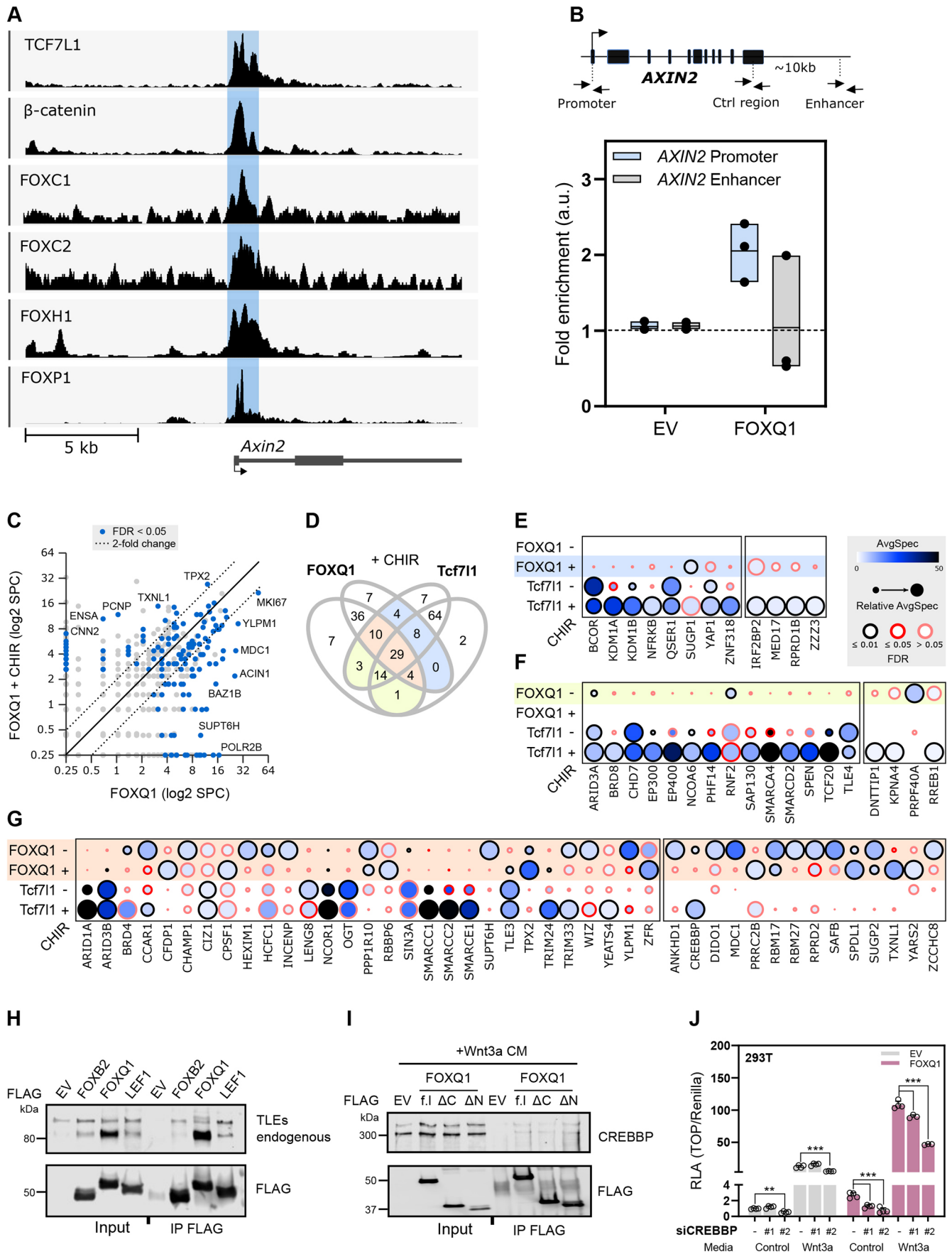


Fig. 5. See next page for legend.

Fig. 5. FOXQ1 occupies Wnt-responsive elements at Wnt target genes and shares multiple transcription co-factors with TCF/LEF. (A) Genomic tracks showing protein-DNA binding enrichment of Tcf711, β -catenin, FOXC1, FOXC2, FOXH1 and FOXP1 at the *Axin2* locus, obtained by ChIP-seq. Data were retrieved from publicly available datasets (references and accession numbers in Fig. S4D). (B) ChIP followed by qPCR in 293T cells upon overexpression of FOXQ1. Enrichment was identified at a Wnt-responsive element in the *AXIN2* promoter, but not at the enhancer or control regions indicated in the schematic above. The data are normalized to immunoprecipitation performed in cells transfected with an empty vector and presented as the mean \pm s.d. of $n=3$ independent experiments. (C) Dot plot highlighting changes in the FOXQ1 proximity interactome upon CHIR treatment. SPC, normalised spectral count. (D) Venn diagram illustrating the proximity interactome overlap between FOXQ1 and Tcf711 (untreated/CHIR99021-treated conditions). Coloured areas indicate shared interactors. (E-G) Dot plot analysis showing the 73 proteins that are common interactors of FOXQ1 and Tcf711. FOXQ1 experiments were performed with four biological replicates for untreated samples, and three replicates for CHIR-treated samples. AvgSpec, average spectral count; FDR, Bayes false discovery rate. (H) Co-immunoprecipitation assay in nuclear lysates of 293T cells. Overexpressed Flag-tagged proteins were pulled down using a Flag antibody, and endogenous TLEs were detected by immunoblotting. FOXB2 and LEF1 were used as negative and positive controls, respectively. Data show results from one experiment. (I) Co-immunoprecipitation from nuclear lysates of 293T cells treated with Wnt3a-conditioned media. Flag-tagged FOXQ1 constructs were pulled down and endogenous CREBBP protein was detected by immunoblot. All FOXQ1 constructs interacted with CREBBP. Data show results from $n=2$ independent experiments. (J) TOPflash in 293T cells after RNA interference of CREBBP. FOXQ1-dependent TOPflash activity was significantly reduced by silencing of CREBBP. Data show one representative of $n=3$ independent experiments. Data are displayed as mean \pm s.d. and statistical significance was determined by Dunnett's post-hoc test following ANOVA (** $P<0.01$, *** $P<0.001$).

MATERIALS AND METHODS

Plasmid/expression construct cloning

Molecular cloning of Flag/V5-tagged FOXQ1, FOXB2 and LEF1 has been described previously (Moparthi et al., 2019). Flag/V5-tagged TCF7L2 and Flag-tagged FOXQ1 truncation constructs were generated by restriction cloning using the high-fidelity Q5 polymerase (New England Biolabs). The FOXQ1 promoter construct was created by cloning a 2.5 kb region of the human FOXQ1 promoter into a pTA-Luc vector backbone.

For cloning of FOXQ1 truncation constructs, the following primers were used: FOXQ1 Δ C- fw, 5'-CATGGAATCAAGTTGGAGGTGTTTCGTCCTCG-3'; FOXQ1 Δ C- rv, 5'-CATGCTCGAGTCAGCGCTTGCGGCGCGGCG-3'; FOXQ1 Δ N- fw, 5'-CATGGAATCAAGCCCCCTACTCGTACATC-3'; and FOXQ1 Δ N- rv, 5'-CATGCTCGAGGCGCTACTCAGGCTAGGAGCGT-3'.

Flag-tagged TurboID was cloned to the N terminus of FOXQ1 for proximity proteomics. All plasmids were validated by partial sequencing (Eurofins Genomics). Additional plasmids used in this study included Flag-LRP6 Δ E1-4 (a gift from Christof Niehrs, Institute of Molecular Biology, Mainz, Germany; Davidson et al., 2005), mCherry-Beta-Catenin-20 (Addgene plasmid 55001, deposited by Michael Davidson, Florida State University, Florida, USA), pcDNA3-S33Y β -catenin (Kolligs et al., 1999; Addgene plasmid 19286, deposited by Eric Fearon, University of Michigan, Ann Arbor, USA) and LEF1 Δ N-VP16 (a gift from Andreas Hecht, University of Freiburg, Freiburg, Germany; Aoki et al., 1999).

Cell culture and transfection

Authenticated 293T, HCT116 and SW48 cells were obtained from the German Collection of Microorganisms and Cell Cultures (DSMZ) and cultured in DMEM (Fisher Scientific) medium supplemented with 10% fetal bovine serum (FBS), 2 mM glutamine and 1% (v/v) penicillin/streptomycin at 37°C and 5% CO₂. Caco-2 cells were from the European Collection of Authenticated Cell Cultures (ECACC), and maintained in DMEM with 15% FBS, 2 mM L-glutamine and 1% (v/v) penicillin/streptomycin. DLD-1 cells were a kind gift from Dr Xiao-Feng Sun (Linköping University, Sweden). These cells were cultured in McCoy's 5A (Fisher Scientific) media

supplemented with 10% FBS and 1% (v/v) penicillin/streptomycin. 293T Δ LRP6, 293T Δ CTNNB1 and 293T penta-knockout cells have been described previously (Doupas et al., 2019; Moparthi et al., 2019).

293T Δ LRP5/6 cells were generated by transfecting 293T Δ LRP6 with an enhanced specificity Cas9 plasmid [eSpCas9(1.1); Slaymaker et al., 2016; Addgene plasmid 71814, deposited by Feng Zhang, Broad Institute of MIT and Harvard, Cambridge, USA] targeting LRP5 (gRNA: 5'-GGAAACTGGAAGTCCACTG-3'). Clonal cell lines were isolated by limiting dilution, and loss-of-function of LRP5/6 was validated by immunoblotting and functional assays, as before (Kirsch et al., 2017).

All cell lines were used at low passage and tested negative for *Mycoplasma* by analytical qPCR (Eurofins Genomics). Wnt3a and control conditioned media were obtained from stably transfected L-cells, following the supplier's guidelines (ATCC). R-spondin 3-conditioned media were generated by transient transfection of Rspo3 Δ C (Ohkawara et al., 2011) into 293T cells. Wnt3a and Rspo3 conditioned media were typically used at 1:4 and 1:1000 dilution, respectively. Cell transfection was performed using Lipofectamine 2000 (Thermo Fisher) or jetOPTIMUS transfection reagents (Polyplus Transfection), according to the supplier's recommendations.

Cas9-mediated transcription activation or inhibition

dCas9-VP64-p65-Rta and dCas9-KRAB-MeCP2 constructs for transcriptional programming (Chavez et al., 2015; Yeo et al., 2018; Addgene plasmids 63798 and 110821, deposited by George Church, Harvard Medical School, Massachusetts, USA) were used for CRISPRa/i. The constructs were guided to non-overlapping loci in the *FOXQ1* promoter using four guide RNAs (gRNAs). The following oligo duplexes were cloned into the BPK1520 expression vector (Kleinstiver et al., 2015; Addgene plasmid 65777, deposited by Keith Joung, Harvard Medical School, Massachusetts, USA) to generate the gRNAs (g1-g4): g1-fw, 5'-caccCCAACGGGCGCGCACCAGG-3'; g1-rv, 5'-aacCCTGGTGC-GCGCCCGTTGGG-3'; g2-fw, 5'-caccGCGCGCCCGTTGGGGAGCTG-3'; g2-rv, 5'-aacCAGTCCCCAACGGGCGCGC-3'; g3-fw, 5'-caccGAGCGCGGACGGCAAGGGT-3'; g3-rv, 5'-aacACCCTTGCCGTC-CGCGCTC-3'; g4-fw, 5'-caccCTGGGGAGCCGCCACCACCT-3'; and g4-rv, 5'-aacAGGTGGTGGCGGCTCCCCAG-3'.

For validation of induction of *FOXQ1* expression, cells were transfected in 24-well plates with 200 ng of dCas9-VPR and 10 ng gRNA in each well. RNA isolation was performed 48 h after transfection. For reporter assays, cells were transfected in 96-well plates with 50 ng of dCas9-VPR or dCas9-KRAB-MeCP2, 5 ng gRNA, 50 ng of the TOPflash β -catenin/TCF reporter (M50 Super 8x TOPflash; Addgene plasmid 12456, deposited by Randall Moon, University of Washington, School of Medicine, Seattle, USA; Veeman et al., 2003) and 5 ng of Renilla luciferase control plasmid (Addgene plasmid 12179, deposited by David Bartel, Whitehead Institute for Biomedical Research, Cambridge, USA) in each well. Cells were grown for 24 h before luminescence measurement.

Small interfering RNA

Scrambled and small interfering RNAs (siRNAs) against human CREBBP were obtained from Integrated DNA Technologies. CREBBP siRNAs were validated by immunoblot. HEK293T cells were transfected with 20 nM siRNAs using Lipofectamine 2000 (Thermo Fisher).

Reporter assays

For the TOPflash assays, cells were seeded on a 96-well plate and transfected with 50 ng TOPflash reporter, 5 ng Renilla luciferase and 10 ng of plasmid of interest in each well. Where indicated, 6 h after transfection cells were treated with control, Wnt3a or Rspo3-conditioned media. For forkhead reporter and FOXQ1 promoter assays, the TOPflash plasmid was replaced with 10x UFR-luc (Moparthi and Koch, 2020) or the promoter constructs described above. The dual luciferase assay was conducted as described previously (Hampf and Gossen, 2006) with a few changes. Briefly, after overnight incubation, cells were lysed in passive lysis buffer [25 mM Tris, 2 mM DTT, 2 mM EDTA, 10% (v/v) glycerol and 1% (v/v) Triton X-100 (pH 7.8)] and agitated for 10 min. Lysates were transferred to a flat-bottomed 96-well luminescence assay plate. Firefly luciferase buffer [200 μ M D-luciferin in 200 mM Tris-HCl, 15 mM MgSO₄, 100 μ M EDTA, 1 mM ATP, 25 mM DTT (pH 8.0)] was added to

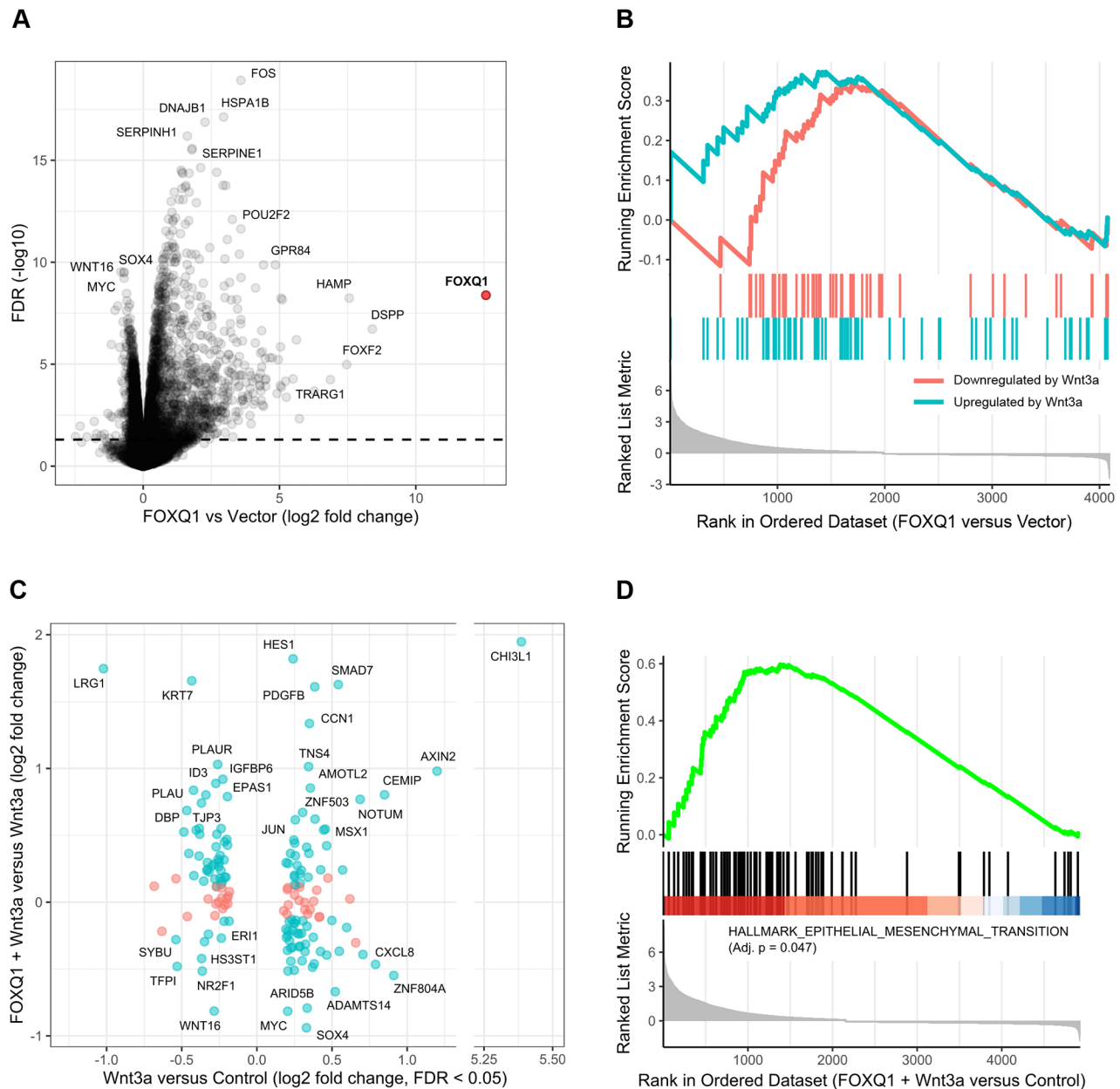


Fig. 6. FOXQ1 alters the transcriptome of colorectal cancer cells. (A) Volcano plot of differentially expressed protein-coding genes in HCT116 cells transfected with FOXQ1, as determined by bulk RNA sequencing (RNA-seq, $n=3$ biological replicates per condition). Some genes of interest are highlighted. The dashed line indicates an FDR of 0.05. (B) Gene set enrichment analysis (GSEA) indicated a modest enrichment for genes regulated by Wnt3a in HCT116. Input genes were derived by RNA-seq of HCT116 treated with recombinant human Wnt3a ($n=3$ per condition, $FDR < 0.05$). (C) Overexpression of FOXQ1 considerably altered the expression of genes differentially regulated by Wnt3a. Genes in cyan had an $FDR < 0.05$ in the FOXQ1+Wnt3a versus Wnt3a comparison. (D) GSEA using the hallmark gene set for epithelial-to-mesenchymal transition. Genes induced by concomitant overexpression of FOXQ1 and Wnt3a treatment were significantly enriched for EMT-related genes. Adj. p , adjusted P -value (Benjamini–Hochberg correction).

each well and the plate was incubated for 2 min at room temperature. Luciferase activity was measured using a Spark10 (Tecan) or a SpectraMax iD3 Multi-Mode Microplate Reader (Molecular Devices). Next, Renilla luciferase buffer [4 μ M coelenterazine-h in 500 mM NaCl, 500 mM Na_2SO_4 , 10 mM NaOAc, 15 mM EDTA, 25 mM sodium pyrophosphate and 50 μ M phenylbenzothiazole (pH 5.0)] was added to the plate and luminescence was measured immediately. Data were normalized to the corresponding Renilla control value in each well.

Antibodies and reagents

The following antibodies were used: mouse anti-Flag M2 (F3165, 1:2000) and rabbit anti-FLAG (F7425, 1:2000) from Sigma Aldrich (St Louis, USA); rabbit anti-non phospho (Active) β -catenin (8814, 1:1000), rabbit anti-TLE1/2/3/4

(4681, 1:1000), rabbit anti-V5 (13202, 1:1000) and rabbit anti-CBP (7389, 1:1000) from Cell Signaling Technology; mouse anti-V5 (ASJ-10004-100, 1:5000) from Nordic Biosite (Täby, Sweden); rabbit anti-HSP70 (AF1663, 1:2000) from R&D Systems; and mouse anti- α tubulin (#NB100-690, 1:5000) and rabbit anti-HA (#NB600-363, 1:2000) from Novus Biologicals.

Chemicals and inhibitors were from Sigma Aldrich and Cayman Chemicals. CHIR99021, LGK974 and XAV939 have been characterised previously (Kulak et al., 2015; Liu et al., 2013; Naujok et al., 2014). Recombinant human WNT3A and R-spondin 3 were from R&D Systems.

Immunocytochemistry

For FOXQ1 deletion construct localization experiments, HCT116 cells were seeded on coverslips in 24-well plates. Cells were transfected with 200 ng of

Flag-tagged FOXQ1 deletion constructs using Lipofectamine 2000 (Thermo Fisher). After 24 h, cells were fixed with 4% paraformaldehyde, permeabilized with 0.1% Triton X-100 in PBS, and blocked with 2% bovine serum albumin (BSA) and 0.1% Tween-20 for 1 h. Mouse anti-Flag M2 was detected using fluorophore-labelled secondary antibodies (Thermo Fisher). Samples were mounted with Hoechst 33342 counterstain for nuclear visualization. Images were acquired on a Leica DMi8 and processed in ImageJ v1.52h.

Quantitative real-time PCR

RNA extraction was performed using a Qiagen RNeasy mini kit and reverse transcribed (RT) with a Thermo Fisher cDNA synthesis kit. cDNA was amplified using validated custom primers, with SYBR green dye. Data were acquired on a Bio-Rad CFX96 Touch thermocycler and normalized to *HPRT1* control. Data are displayed as fold change compared with empty vector control and show biological triplicates with technical duplicates. The raw data for all qPCR experiments are included in Table S4.

Immunoblotting and immunoprecipitation

Cells were harvested in PBS and lysed in lysis buffer (0.1-1% NP-40 in PBS with 1× protease inhibitor cocktail). Lysates were boiled in Laemmli sample buffer with 50 mM DTT, separated on 10% polyacrylamide gels (Bio-Rad), transferred onto nitrocellulose membranes and incubated in blocking buffer (LI-COR). Primary antibodies were detected using near-infrared (NIR) fluorophore-labelled secondary antibodies (1:20,000, cat. no. 926-68072 and 926-32213; LI-COR). Blots were scanned on a LI-COR CLx imager.

For co-immunoprecipitation experiments, cells were seeded in 6-well plates and transfected with approximately 1 µg of the indicated constructs per well. Cells were harvested in PBS and nuclear extraction was performed using 0.1% NP-40 in PBS with 1× protease inhibitor cocktail. The proteins were pre-cleared using protein A/G agarose beads and immunoprecipitated using anti-Flag M2 Affinity Gel beads (A2220, Sigma Aldrich) overnight in a cold room. Samples were washed three times with 0.1% NP-40 in PBS, eluted in Laemmli buffer and used for immunoblotting. All of the uncropped blot images are provided in Fig. S7.

TurboID and mass spectrometry

The labelling and sample preparation of TurboID experiments was performed as described previously (Branon et al., 2018). Briefly, N-terminal TurboID-FOXQ1 and TurboID plasmids were transiently transfected into 293T cells using jetOPTIMUS (Polyplus Transfection). After 21 h of transfection, cells were treated with 500 µM biotin and incubated for 3 h at 37°C in 5% CO₂. For Wnt signalling activation, cells were treated after 6 h from transfection with 5 µM CHIR99021 and incubated for 15 h before the addition of biotin. Cells were surface washed with ice-cold PBS three times to remove excess biotin and then harvested by centrifuging at 480 g for 15 min. Cells were washed thrice with ice-cold PBS buffer by centrifugation to remove any remaining biotin. Cells were lysed in RIPA buffer containing 1× protease inhibitor cocktail for 15 min on ice. Pre-washed streptavidin beads (GE Healthcare) were added to the cell lysate and incubated overnight at 4°C with end-over-end rotation. The beads were washed once with 1 ml of RIPA buffer, once with 1 ml of 1 M KCl, once with 1 ml of 0.1 M Na₂CO₃, once with 1 ml of 2 M urea in 10 mM Tris-HCl (pH 8.0) and twice with 1 ml RIPA lysis buffer. The beads were then transferred to a new Eppendorf tube and washed twice with 50 mM Tris-HCl buffer (pH 7.5) and 2 M urea/50 mM Tris (pH 7.5) buffer. Beads were incubated with 0.4 µg trypsin (Thermo Fisher Scientific) in 2 M urea/50 mM Tris containing 1 mM DTT for 1 h at 25°C with end-over-end rotation. After incubation, the supernatant was collected and the beads were washed twice with 60 µl of 2 M urea/50 mM Tris buffer (pH 7.5) and the washes were combined with the collected supernatant. The supernatant was reduced with 4 mM DTT for 30 min at 25°C with end-over-end rotation. The samples were alkylated with 10 mM iodoacetamide for 45 min in the dark at 25°C with end-over-end rotation. For the complete digestion of the sample, an additional 0.5 µg of trypsin was added and incubated at 25°C overnight with end-over-end rotation. After overnight digestion, the samples were desalted with C18 Pipette tips (Thermo Fisher Scientific) and then dried with a vacuum centrifuge.

TurboID samples were analysed by mass spectrometry, using an Easy nano LC 1200 system interfaced with a nanoEasy spray ion source (Thermo Fisher Scientific) connected to the Q Exactive HF Hybrid Quadrupole-Orbitrap Mass Spectrometer (Thermo Fisher Scientific). The peptides were loaded on a pre-column (Acclaim PepMap 100, 75 µm×2 cm, Thermo Fisher Scientific) and the chromatographic separation was performed using an EASY-Spray C18 reversed-phase nano LC column (PepMap RSLC C18, 2 µm, 100A 75 µm×25 cm, Thermo Fisher Scientific). The nanoLC was operating at 300 nl/min flow rate with a gradient (6-40% in 95 min and 5 min hold at 100%) of solvent B [0.1% (v/v) formic acid in 100% acetonitrile] in solvent A [0.1% (v/v) formic acid in water] for 100 min.

Separated peptides were electrosprayed and analysed using a Q-Exactive HF mass spectrometer (Thermo Fisher Scientific), operated in positive polarity in a data-dependent mode. Full scans were performed at 120,000 resolutions at a range of 380-1400 m/z. The top 15 most intense multiple charged ions were isolated (1.2 m/z isolation window) and fragmented at a resolution of 30,000 with a dynamic exclusion of 30.0 s.

Raw data were processed by Proteome Discoverer 1.4 (Thermo Fisher Scientific) searching against the *Homo sapiens* UniProt database (release from 2019-12-16) with Sequest HT search engine. The search parameters were: taxonomy, *Homo sapiens*; enzymes, trypsin with two missed cleavages; no variable modifications; fixed modification, carbamidomethyl; peptide mass tolerance, 10 ppm; MS/MS fragment tolerance, 0.02 Da (0.1 Da for CHIR-treated samples). Quantification of the analysed data was performed with Scaffold 5.1.0 (Proteome Software), a Proteome Software using total spectral count. Protein identifications that were accepted contained at least two identified peptides and probability >95%. Peptide identifications were accepted if they could be established at >90% probability by the Scaffold Local FDR algorithm.

TurboID data analysis

Proteins indicated in the Proteome Discoverer output files as significantly increased in the TurboID-FOXQ1 samples (Fisher's exact test<0.05) were subjected to gene ontology analysis in DAVID v6.8 (Jiao et al., 2012), using the 'BP Direct' function with default options. Processed mass spectrometry data were analysed further using SAINTexpress v3.6.3 (Teo et al., 2014). The resulting output files were merged with a dataset of Tcf711 interactors in mouse embryonic stem cells (Moreira et al., 2018 preprint), following mouse-to-human gene name conversion using the biomaRt R package (Durinck et al., 2009). Data were filtered against common mass spectrometry contaminants using the CRAPome repository (Mellacheruvu et al., 2013) with Frequency cut-off 0.2 or PSM ratio cut-off 3. Data were then analysed and visualised in ProHits-viz (Knight et al., 2017), using the Dot plot analysis tool with default options.

RNA-sequencing

HCT116 cells were treated with 10 nM LGK974 and transiently transfected with empty vector or FOXQ1. After transfection, cells were treated overnight with 100 ng/ml recombinant human WNT3A protein (R&D Systems). Each condition was performed in biological triplicates. Total RNA was isolated after 24 h from transfection using a Qiagen RNeasy mini kit and library preparation was performed using the NEBNext RNA Library Prep Kit. RNA and cDNA quality were assessed using the 2100 Bioanalyzer instrument (Agilent) and the Fragment analyzer System (Agilent), respectively. The libraries were sequenced using the NextSeq 550 Sequencing System (Illumina) at the Core facility of Linköping University.

RNA-sequencing data analysis

Raw reads quality was assessed using FastQC (v0.11.9) (Andrews, 2010). STAR (v2.7.6a) (Dobin et al., 2013) was used to map the reads against the human genome (genome assembly GRCh38 release 106, http://ftp.ensembl.org/pub/release-106/fasta/homo_sapiens/dna/Homo_sapiens.GRCh38.dna.primary_assembly.fa.gz; annotation, http://ftp.ensembl.org/pub/release-106/gtf/homo_sapiens/Homo_sapiens.GRCh38.106.gtf.gz) and the resulting BAM files were sorted by coordinates (parameter: -outSAMtype BAM

SortedByCoordinate). Reads count was performed using featureCounts (v2.0.1) (Liao et al., 2014) generating gene counts (parameter: -g gene_id). Differential gene expression analysis of the processed data was performed using edgeR v3.38.1 (Robinson et al., 2009). Gene ontology (GO), biological processes (BP) and gene set enrichment analyses (GSEA) and visualisation were carried out using clusterProfiler v4.4.4 and enrichplot v1.16.1 (Wu et al., 2021). Hallmark gene sets were from the Molecular Signatures Database v7.5.1 (Liberzon et al., 2015). The gene set of β -catenin target genes in CRC cells was from Herbst et al. (2014), excluding downregulated genes. Microarray data of shFOXQ1 or control transfected DLD-1 cells (GSE74223; Tang et al., 2020) were accessed through the GEOquery R package implemented in the GEO2R web tool (<https://www.ncbi.nlm.nih.gov/geo/geo2r/>), using default options.

Forkhead box phylogenetic analysis

FOX transcription factor phylogenetic tree was constructed using the Molecular Evolutionary Genetics Analysis (MEGA) software (version 11) (Tamura et al., 2021). Forkhead box domain peptide sequences for each FOX transcription factor were downloaded from the UniProt database (UniProt Consortium, 2021) (accessed 2021-12-14). Multiple sequence alignment was performed using the ClustalW algorithm with default settings. Phylogenetic analysis and construction of Maximum Likelihood Phylogenetic Tree was carried out with default settings.

External Chip-seq data

We performed a systematic review of publicly available FOX transcription factor ChIP-seq data from mouse. Datasets were downloaded from the Gene Expression Omnibus (GEO) database. Data based on older versions of the mouse reference genome were converted to version mm10 using the UCSC liftOver tool. Data files were further converted to BigWig file format before visualization in the Integrative Genomics Viewer (IGV) (Robinson et al., 2011).

In silico FOXQ1 binding prediction

FOXQ1 transcription factor-binding profile data were downloaded from the JASPAR database, 9th release (2022) (Castro-Mondragon et al., 2021) as position frequency matrices (PFMs). Based on these binding profiles, FOXQ1 binding was predicted at the *Axin2* and *Lef1* loci (mouse reference genome mm10) using the R package TFBStools (Tan and Lenhard, 2016). Genomic regions in which to scan for FOXQ1 binding patterns were defined so as to include sites previously identified as Wnt-responsive elements (WRE) (Jho et al., 2002; Li et al., 2006).

Chromatin immunoprecipitation

293T cells (5×10^7) were crosslinked in 20 ml PBS for 40 min with the addition of 1.5 mM ethylene glycol-bis (succinimidyl succinate) (Thermo Scientific), for protein-protein crosslinking (Salazar et al., 2019), and 1% formaldehyde for the last 20 min of incubation, to preserve DNA-protein interactions. The reaction was blocked with glycine and the cells were subsequently lysed in 1 ml HEPES buffer (0.3% SDS, 1% Triton-X 100, 0.15 M NaCl, 1 mM EDTA, 0.5 mM EGTA and 20 mM HEPES). Chromatin was sheared using Covaris S220 for 4 min with the following set up: duty factor, 20.0; peak power, 200.0; cycles/burst, 1000 (Covaris SonoLab 7.2). The sonicated chromatin was diluted twice to 0.15% SDS and cell debris were discarded by centrifugation at 10,000 *g* for 1 min. The chromatin was incubated overnight at 4°C with 50 μ l anti-Flag M2 beads (Sigma Aldrich). The beads were washed at 4°C with wash buffer 1 (0.1% SDS, 0.1% deoxycholate, 1% Triton X-100, 0.15 M NaCl, 1 mM EDTA, 0.5 mM EGTA and 20 mM HEPES), wash buffer 2 (0.1% SDS, 0.1% sodium deoxycholate, 1% Triton X-100, 0.5 M NaCl, 1 mM EDTA, 0.5 mM EGTA and 20 mM HEPES), wash buffer 3 (0.25 M LiCl, 0.5% sodium deoxycholate, 0.5% NP-40, 1 mM EDTA, 0.5 mM EGTA and 20 mM HEPES) and, finally, twice with Tris EDTA buffer (all washing solution were kept at 4°C). The chromatin was eluted with 1% SDS, 0.1 M NaHCO₃, de-crosslinked by incubation at 65°C for 5 h with 200 mM NaCl, extracted with phenol-chloroform and ethanol precipitated. The immunoprecipitated DNA was used for quantitative PCR using primers previously described (Zimmerli et al., 2020).

MTT assay

HCT116 and 293T cells were seeded into 96-well plates at a density of 5×10^3 cells/well and transfected with 50 ng plasmids/well using jetOPTIMUS transfection reagents (Polyplus Transfection). Cell proliferation was evaluated at different time points from transfection using the MTT Cell Growth Assay kit (Merck Millipore). Absorbance was measured on a SpectraMax iD3 Multi-Mode Microplate Reader (Molecular Devices), using a test wavelength of 570 nm and a reference wavelength of 630 nm.

Statistical analyses

Data are shown as mean with standard deviation (s.d.). Each experiment included controls (e.g. empty backbone plasmid, scrambled siRNA and substance carriers) at identical concentrations. Statistical tests are indicated in the figure legends, and were carried out in R 4.1.1 or GraphPad Prism 8.4.

Acknowledgements

The authors thank all investigators who have made data and materials available to the scientific community, Dr Xiao-Feng Sun (Linköping University) for providing the DLD-1 cell line, and Dr Andreas Hecht (University of Freiburg) for the LEF1 Δ N-VP16 construct. We acknowledge the Core Facility at the Faculty of Medicine and Health Sciences of Linköping University for providing assistance with bioinformatics, molecular biology and mass spectrometry.

Competing interests

The authors declare no competing or financial interests.

Author contributions

Conceptualization: L.M., S.K.; Methodology: G.P., L.M., S.S., C.C.; Formal analysis: G.P., L.M., S.S., S.K.; Investigation: G.P., L.M., S.S., C.C.; Resources: L.M., C.C., S.K.; Data curation: L.M., S.K.; Writing - original draft: G.P.; Writing - review & editing: L.M., S.S., C.C., S.K.; Visualization: G.P., S.S.; Supervision: C.C., S.K.; Funding acquisition: C.C., S.K.

Funding

S.K. and C.C. are Wallenberg Molecular Medicine Fellows and receive financial support from the Knut och Alice Wallenbergs Stiftelse (long-term fellowship support). Additional financial support came from project grants from the Vetenskapsrådet (2020-01084 to S.K.) and from Cancerfonden (20 0737 Pj 01 H to S.K. and CAN 2018/542 to C.C.). Open access funding provided by Linköpings Universitet. Deposited in PMC for immediate release.

Data availability

The mass spectrometry proteomics data have been deposited to the ProteomeXchange Consortium via the PRIDE partner repository with the dataset identifier PXD030464 (FOXQ1 samples) and PXD035624 (FOXQ1+CHIR samples). The RNA-sequencing data have been deposited in the ArrayExpress database at EMBL-EBI (<http://www.ebi.ac.uk/arrayexpress>) under accession number E-MTAB-12062.

Peer review history

The peer review history is available online at <https://journals.biologists.com/jcs/lookup/doi/10.1242/jcs.260082.reviewer-comments.pdf>.

References

- Abba, M., Patil, N., Rasheed, K., Nelson, L. D., Mudduluru, G., Leupold, J. H. and Allgayer, H. (2013). Unraveling the role of FOXQ1 in colorectal cancer metastasis. *Mol. Cancer Res.* **11**, 1017-1028. doi:10.1158/1541-7786.MCR-13-0024
- Andrews, S. (2010). *FastQC: A Quality Control Tool for High Throughput Sequence Data: Babraham Bioinformatics*. Cambridge, UK: Babraham Institute.
- Aoki, M., Hecht, A., Kruse, U., Kemler, R. and Vogt, P. K. (1999). Nuclear endpoint of Wnt signaling: neoplastic transformation induced by transactivating lymphoid-enhancing factor 1. *Proc. Natl Acad. Sci. USA* **96**, 139-144. doi:10.1073/pnas.96.1.139
- Bagati, A., Bianchi-Smiraglia, A., Moparthy, S., Kolesnikova, K., Fink, E. E., Lipchick, B. C., Kolesnikova, M., Jowdy, P., Polechetti, A., Mahpour, A. et al. (2017). Melanoma suppressor functions of the carcinoma oncogene FOXQ1. *Cell Rep.* **20**, 2820-2832. doi:10.1016/j.celrep.2017.08.057
- Barker, N., Hurlstone, A., Musisi, H., Miles, A., Bienz, M. and Clevers, H. (2001). The chromatin remodelling factor Brg-1 interacts with beta-catenin to promote target gene activation. *EMBO J.* **20**, 4935-4943. doi:10.1093/emboj/20.17.4935

- Basu, S., Haase, G. and Ben-Ze'ev, A. (2016). Wnt signaling in cancer stem cells and colon cancer metastasis. *F1000Res* **5**, 699. doi:10.12688/f1000research.7579.1
- Branon, T. C., Bosch, J. A., Sanchez, A. D., Udeshi, N. D., Svinkina, T., Carr, S. A., Feldman, J. L., Perrimon, N. and Ting, A. Y. (2018). Efficient proximity labeling in living cells and organisms with TurboID. *Nat. Biotechnol.* **36**, 880-887. doi:10.1038/nbt.4201
- Byles, V., Zhu, L., Lovaas, J. D., Chmielewski, L. K., Wang, J., Faller, D. V. and Dai, Y. (2012). SIRT1 induces EMT by cooperating with EMT transcription factors and enhances prostate cancer cell migration and metastasis. *Oncogene* **31**, 4619-4629. doi:10.1038/onc.2011.612
- Castro-Mondragon, J. A., Riudavets-Puig, R., Rauluseviciute, I., Berhanu Lemma, R., Turchi, L., Blanc-Mathieu, R., Lucas, J., Boddie, P., Khan, A., Manosalva Perez, N. et al. (2021). JASPAR 2022: the 9th release of the open-access database of transcription factor binding profiles. *Nucleic Acids Res.* **50**, D165-D173. doi:10.1093/nar/gkab1113
- Chavez, A., Scheiman, J., Vora, S., Pruitt, B. W., Tuttle, M., Iyer, E. P. R., Lin, S., Kiani, S., Guzman, C. D., Wiegand, D. J. et al. (2015). Highly efficient Cas9-mediated transcriptional programming. *Nat. Methods* **12**, 326-328. doi:10.1038/nmeth.3312
- Cheng, F., Su, L., Yao, C., Liu, L., Shen, J., Liu, C., Chen, X., Luo, Y., Jiang, L., Shan, J. et al. (2016). SIRT1 promotes epithelial-mesenchymal transition and metastasis in colorectal cancer by regulating Fra-1 expression. *Cancer Lett.* **375**, 274-283. doi:10.1016/j.canlet.2016.03.010
- Cho, K. F., Branon, T. C., Udeshi, N. D., Myers, S. A., Carr, S. A. and Ting, A. Y. (2020). Proximity labeling in mammalian cells with TurboID and split-TurboID. *Nat. Protoc.* **15**, 3971-3999. doi:10.1038/s41596-020-0399-0
- Christensen, J., Bentz, S., Sengstag, T., Shastri, V. P. and Anderle, P. (2013). FOXQ1, a novel target of the Wnt pathway and a new marker for activation of Wnt signaling in solid tumors. *PLoS One* **8**, e60051. doi:10.1371/journal.pone.0060051
- Clevers, H. (2006). Wnt/ β -catenin signaling in development and disease. *Cell* **127**, 469-480. doi:10.1016/j.cell.2006.10.018
- Daniels, D. L. and Weis, W. I. (2005). β -catenin directly displaces Groucho/TLE repressors from Tcf/Lef in Wnt-mediated transcription activation. *Nat. Struct. Mol. Biol.* **12**, 364-371. doi:10.1038/nsmb912
- Davidson, G., Wu, W., Shen, J., Bilic, J., Fenger, U., Stannek, P., Glinka, A. and Niehrs, C. (2005). Casein kinase 1 γ couples Wnt receptor activation to cytoplasmic signal transduction. *Nature* **438**, 867-872. doi:10.1038/nature04170
- Dobin, A., Davis, C. A., Schlesinger, F., Drenkow, J., Zaleski, C., Jha, S., Batut, P., Chaisson, M. and Gingeras, T. R. (2013). STAR: ultrafast universal RNA-seq aligner. *Bioinformatics* **29**, 15-21. doi:10.1093/bioinformatics/bts635
- Doumpas, N., Lampart, F., Robinson, M. D., Lentini, A., Nestor, C. E., Cantu, C. and Basler, K. (2019). TCF/LEF dependent and independent transcriptional regulation of Wnt/ β -catenin target genes. *EMBO J.* **38**, e98873. doi:10.15252/embj.201798873
- Durinck, S., Spellman, P. T., Birney, E. and Huber, W. (2009). Mapping identifiers for the integration of genomic datasets with the R/Bioconductor package biomaRt. *Nat. Protoc.* **4**, 1184-1191. doi:10.1038/nprot.2009.97
- Hampf, M. and Gossen, M. (2006). A protocol for combined Photinus and Renilla luciferase quantification compatible with protein assays. *Anal. Biochem.* **356**, 94-99. doi:10.1016/j.ab.2006.04.046
- Herbst, A., Jurinovic, V., Krebs, S., Thieme, S. E., Blum, H., Göke, B. and Kolligs, F. T. (2014). Comprehensive analysis of β -catenin target genes in colorectal carcinoma cell lines with deregulated Wnt/ β -catenin signaling. *BMC Genomics* **15**, 74. doi:10.1186/1471-2164-15-74
- Jho, E.-H., Zhang, T., Domon, C., Joo, C.-K., Freund, J.-N. and Costantini, F. (2002). Wnt/ β -catenin/Tcf signaling induces the transcription of Axin2, a negative regulator of the signaling pathway. *Mol. Cell. Biol.* **22**, 1172-1183. doi:10.1128/MCB.22.4.1172-1183.2002
- Jiao, X., Sherman, B. T., Huang, D. W., Stephens, R., Baseler, M. W., Lane, H. C. and Lempicki, R. A. (2012). DAVID-WS: a stateful web server to facilitate gene/protein list analysis. *Bioinformatics* **28**, 1805-1806. doi:10.1093/bioinformatics/bts251
- Kaneda, H., Arai, T., Tanaka, K., Tamura, D., Aomatsu, K., Kudo, K., Sakai, K., De Velasco, M. A., Matsumoto, K., Fujita, Y. et al. (2010). FOXQ1 is overexpressed in colorectal cancer and enhances tumorigenicity and tumor growth. *Cancer Res.* **70**, 2053-2063. doi:10.1158/0008-5472.CAN-09-2161
- Kirsch, N., Chang, L.-S., Koch, S., Glinka, A., Dolde, C., Colozza, G., Benitez, M. D., De Robertis, E. M. and Niehrs, C. (2017). Angiopoietin-like 4 is a Wnt signaling antagonist that promotes LRP6 turnover. *Dev. Cell* **43**, 71-82.e6. doi:10.1016/j.devcel.2017.09.011
- Kleinstiver, B. P., Prew, M. S., Tsai, S. Q., Topkar, V. V., Nguyen, N. T., Zheng, Z., Gonzales, A. P. W., Li, Z., Peterson, R. T., Yeh, J.-R. J. et al. (2015). Engineered CRISPR-Cas9 nucleases with altered PAM specificities. *Nature* **523**, 481-485. doi:10.1038/nature14592
- Knight, J. D. R., Choi, H., Gupta, G. D., Pelletier, L., Raught, B., Nesvizhskii, A. I. and Gingras, A.-C. (2017). ProHits-viz: a suite of web tools for visualizing interaction proteomics data. *Nat. Methods* **14**, 645-646. doi:10.1038/nmeth.4330
- Koch, S. (2021). Regulation of Wnt signaling by FOX transcription factors in cancer. *Cancers (Basel)* **13**, 3446. doi:10.3390/cancers13143446
- Kolligs, F. T., Hu, G., Dang, C. V. and Fearon, E. R. (1999). Neoplastic transformation of RK3E by mutant β -catenin requires deregulation of Tcf/Lef transcription but not activation of c-myc expression. *Mol. Cell. Biol.* **19**, 5696-5706. doi:10.1128/MCB.19.8.5696
- Kulak, O., Chen, H., Holohan, B., Wu, X., He, H., Borek, D., Otwinowski, Z., Yamaguchi, K., Garofalo, L. A., Ma, Z. et al. (2015). Disruption of Wnt/ β -catenin signaling and telomeric shortening are inextricable consequences of tankyrase inhibition in human cells. *Mol. Cell. Biol.* **35**, 2425-2435. doi:10.1128/MCB.00392-15
- Li, T. W.-H., Ting, J.-H. T., Yokoyama, N. N., Bernstein, A., van de Wetering, M. and Waterman, M. L. (2006). Wnt activation and alternative promoter repression of LEF1 in colon cancer. *Mol. Cell. Biol.* **26**, 5284-5299. doi:10.1128/MCB.00105-06
- Li, J., Sutter, C., Parker, D. S., Blauwkamp, T., Fang, M. and Cadigan, K. M. (2007). CBP/p300 are bimodal regulators of Wnt signaling. *EMBO J.* **26**, 2284-2294. doi:10.1038/sj.emboj.7601667
- Liao, Y., Smyth, G. K. and Shi, W. (2014). featureCounts: an efficient general purpose program for assigning sequence reads to genomic features. *Bioinformatics* **30**, 923-930. doi:10.1093/bioinformatics/btt656
- Liberzon, A., Birger, C., Thorvaldsdóttir, H., Ghandi, M., Mesirov, J. P. and Tamayo, P. (2015). The molecular signatures database hallmark gene set collection. *Cell Syst.* **1**, 417-425. doi:10.1016/j.cels.2015.12.004
- Liu, J., Pan, S., Hsieh, M. H., Ng, N., Sun, F., Wang, T., Kasibhatla, S., Schuller, A. G., Li, A. G., Cheng, D. et al. (2013). Targeting Wnt-driven cancer through the inhibition of Porcupine by LGK974. *Proc. Natl. Acad. Sci. USA* **110**, 20224-20229. doi:10.1073/pnas.1314239110
- Liu, J. Y., Wu, X. Y., Wu, G. N., Liu, F.-K. and Yao, X.-Q. (2017). FOXQ1 promotes cancer metastasis by PI3K/AKT signaling regulation in colorectal carcinoma. *Am. J. Transl. Res.* **9**, 2207-2218.
- MacDonald, B. T., Tamai, K. and He, X. (2009). Wnt/ β -catenin signaling: components, mechanisms, and diseases. *Dev. Cell* **17**, 9-26. doi:10.1016/j.devcel.2009.06.016
- Masuda, T. and Ishitani, T. (2017). Context-dependent regulation of the β -catenin transcriptional complex supports diverse functions of Wnt/ β -catenin signaling. *J. Biochem.* **161**, 9-17. doi:10.1093/jb/mvw072
- Mellacheruvu, D., Wright, Z., Couzens, A. L., Lambert, J.-P., St-Denis, N. A., Li, T., Miteva, Y. V., Hauri, S., Sardi, M. E., Low, T. Y. et al. (2013). The CRAPome: a contaminant repository for affinity purification-mass spectrometry data. *Nat. Methods* **10**, 730-736. doi:10.1038/nmeth.2557
- Moparthy, L. and Koch, S. (2020). A uniform expression library for the exploration of FOX transcription factor biology. *Differentiation* **115**, 30-36. doi:10.1016/j.diff.2020.08.002
- Moparthy, L., Pizzolato, G. and Koch, S. (2019). Wnt activator FOXB2 drives the neuroendocrine differentiation of prostate cancer. *Proc. Natl. Acad. Sci. USA* **116**, 22189-22195. doi:10.1073/pnas.1906484116
- Moreira, S., Seo, C., Gordon, V., Xing, S., Wu, R., Polena, E., Fung, V., Ng, D., Wong, C. J., Larsen, B. et al. (2018). Endogenous BioID elucidates TCF7L1 interactome modulation upon GSK-3 inhibition in mouse ESCs. *bioRxiv*.
- Naujok, O., Lentens, J., Diekmann, U., Davenport, C. and Lenzen, S. (2014). Cytotoxicity and activation of the Wnt/ β -catenin pathway in mouse embryonic stem cells treated with four GSK3 inhibitors. *BMC Res. Notes* **7**, 273. doi:10.1186/1756-0500-7-273
- Nusse, R. and Clevers, H. (2017). Wnt/ β -catenin signaling, disease, and emerging therapeutic modalities. *Cell* **169**, 985-999. doi:10.1016/j.cell.2017.05.016
- Ohkawara, B., Glinka, A. and Niehrs, C. (2011). Rspo3 binds syndecan 4 and induces Wnt/PCP signaling via clathrin-mediated endocytosis to promote morphogenesis. *Dev. Cell* **20**, 303-314. doi:10.1016/j.devcel.2011.01.006
- Ou, C.-Y., Kim, J. H., Yang, C. K. and Stallcup, M. R. (2009). Requirement of cell cycle and apoptosis regulator 1 for target gene activation by Wnt and β -catenin and for anchorage-independent growth of human colon carcinoma cells. *J. Biol. Chem.* **284**, 20629-20637. doi:10.1074/jbc.M109.014332
- Peng, X., Luo, Z., Kang, Q., Deng, D., Wang, Q., Peng, H., Wang, S. and Wei, Z. (2015). FOXQ1 mediates the cross-talk between TGF- β and Wnt signaling pathways in the progression of colorectal cancer. *Cancer Biol. Ther.* **16**, 1099-1109. doi:10.1080/15384047.2015.1047568
- Qiao, Y., Jiang, X., Lee, S. T., Karuturi, R. K. M., Hooi, S. C. and Yu, Q. (2011). FOXQ1 regulates epithelial-mesenchymal transition in human cancers. *Cancer Res.* **71**, 3076-3086. doi:10.1158/0008-5472.CAN-10-2787
- Robinson, M. D., McCarthy, D. J. and Smyth, G. K. (2009). edgeR: a Bioconductor package for differential expression analysis of digital gene expression data. *Bioinformatics* **26**, 139-140. doi:10.1093/bioinformatics/btp616
- Robinson, J. T., Thorvaldsdóttir, H., Winckler, W., Guttman, M., Lander, E. S., Getz, G. and Mesirov, J. P. (2011). Integrative genomics viewer. *Nat. Biotechnol.* **29**, 24-26. doi:10.1038/nbt.1754
- Rodrigues, G., Hoshino, A., Kenific, C. M., Matei, I. R., Steiner, L., Freitas, D., Kim, H. S., Oxley, P. R., Scandariato, I., Casanova-Salas, I. et al. (2019).

- Tumour exosomal CEMIP protein promotes cancer cell colonization in brain metastasis. *Nat. Cell Biol.* **21**, 1403-1412. doi:10.1038/s41556-019-0404-4
- Salazar, V. S., Capelo, L. P., Cantù, C., Zimmerli, D., Gosalia, N., Pregizer, S., Cox, K., Ohte, S., Feigenson, M., Gamer, L. et al.** (2019). Reactivation of a developmental Bmp2 signaling center is required for therapeutic control of the murine periosteal niche. *eLife* **8**, e42386. doi:10.7554/eLife.42386
- Slymaker, I. M., Gao, L., Zetsche, B., Scott, D. A., Yan, W. X. and Zhang, F.** (2016). Rationally engineered Cas9 nucleases with improved specificity. *Science* **351**, 84-88. doi:10.1126/science.aad5227
- Soderholm, S. and Cantu, C.** (2020). The WNT/ β -catenin dependent transcription: a tissue-specific business. *Wiley Interdiscip. Rev. Syst. Biol. Med.* **13**, e1511. doi:10.1002/wsbm.1511
- Subramanian, A., Tamayo, P., Mootha, V. K., Mukherjee, S., Ebert, B. L., Gillette, M. A., Paulovich, A., Pomeroy, S. L., Golub, T. R., Lander, E. S. et al.** (2005). Gene set enrichment analysis: a knowledge-based approach for interpreting genome-wide expression profiles. *Proc. Natl Acad. Sci. USA* **102**, 15545-15550. doi:10.1073/pnas.0506580102
- Tamura, K., Stecher, G. and Kumar, S.** (2021). MEGA11: Molecular Evolutionary Genetics Analysis Version 11. *Mol. Biol. Evol.* **38**, 3022-3027. doi:10.1093/molbev/msab120
- Tan, G. and Lenhard, B.** (2016). TFBSTools: an R/bioconductor package for transcription factor binding site analysis. *Bioinformatics* **32**, 1555-1556. doi:10.1093/bioinformatics/btw024
- Tang, H., Zheng, J., Bai, X., Yue, K.-L., Liang, J.-H., Li, D.-Y., Wang, L.-P., Wang, J.-L. and Guo, Q.** (2020). Forkhead Box Q1 is critical to angiogenesis and macrophage recruitment of colorectal cancer. *Front. Oncol.* **10**, 564298. doi:10.3389/fonc.2020.564298
- Teo, G., Liu, G., Zhang, J., Nesvizhskii, A. I., Gingras, A.-C. and Choi, H.** (2014). SAINTexpress: improvements and additional features in Significance Analysis of INTeractome software. *J. Proteomics* **100**, 37-43. doi:10.1016/j.jprot.2013.10.023
- UniProt Consortium.** (2021). UniProt: the universal protein knowledgebase in 2021. *Nucleic Acids Res.* **49**, D480-D489. doi:10.1093/nar/gkaa1100
- Veeman, M. T., Slusarski, D. C., Kaykas, A., Louie, S. H. and Moon, R. T.** (2003). Zebrafish prickles, a modulator of noncanonical Wnt/Fz signaling, regulates gastrulation movements. *Curr. Biol.* **13**, 680-685. doi:10.1016/S0960-9822(03)00240-9
- Walker, M. P., Stopford, C. M., Cederlund, M., Fang, F., Jahn, C., Rabinowitz, A. D., Goldfarb, D., Graham, D. M., Yan, F., Deal, A. M. et al.** (2015). FOXP1 potentiates Wnt/ β -catenin signaling in diffuse large B cell lymphoma. *Sci. Signal.* **8**, ra12. doi:10.1126/scisignal.2005654
- Wang, W., Li, X., Lee, M., Jun, S., Aziz, K. E., Feng, L., Tran, M. K., Li, N., McCrea, P. D., Park, J.-I. et al.** (2015). FOXKs promote Wnt/ β -catenin signaling by translocating DVL into the nucleus. *Dev. Cell* **32**, 707-718. doi:10.1016/j.devcel.2015.01.031
- Weng, W., Okugawa, Y., Toden, S., Toiyama, Y., Kusunoki, M. and Goel, A.** (2016). FOXM1 and FOXQ1 are promising prognostic biomarkers and novel targets of Tumor-Suppressive miR-342 in human colorectal cancer. *Clin. Cancer Res.* **22**, 4947-4957. doi:10.1158/1078-0432.CCR-16-0360
- Wu, Z.-Q., Brabletz, T., Fearon, E., Willis, A. L., Hu, C. Y., Li, X.-Y. and Weiss, S. J.** (2012). Canonical Wnt suppressor, Axin2, promotes colon carcinoma oncogenic activity. *Proc. Natl Acad. Sci. USA* **109**, 11312-11317. doi:10.1073/pnas.1203015109
- Wu, T., Hu, E., Xu, S., Chen, M., Guo, P., Dai, Z., Feng, T., Zhou, L., Tang, W., Zhan, L. et al.** (2021). clusterProfiler 4.0: a universal enrichment tool for interpreting omics data. *Innovation* **2**, 100141. doi:10.1016/j.xinn.2021.100141
- Xiang, L., Zheng, J., Zhang, M., Ai, T. and Cai, B.** (2020). FOXQ1 promotes the osteogenic differentiation of bone mesenchymal stem cells via Wnt/ β -catenin signaling by binding with ANXA2. *Stem Cell Res. Ther.* **11**, 403. doi:10.1186/s13287-020-01928-9
- Yaklichkin, S., Vekker, A., Stayrook, S., Lewis, M. and Kessler, D. S.** (2007). Prevalence of the EH1 Groucho interaction motif in the metazoan Fox family of transcriptional regulators. *BMC Genomics* **8**, 201. doi:10.1186/1471-2164-8-201
- Yang, M., Liu, Q., Dai, M., Peng, R., Li, X., Zuo, W., Gou, J., Zhou, F., Yu, S., Liu, H. et al.** (2022). FOXQ1-mediated SIRT1 upregulation enhances stemness and radio-resistance of colorectal cancer cells and restores intestinal microbiota function by promoting β -catenin nuclear translocation. *J. Exp. Clin. Cancer Res.* **41**, 70. doi:10.1186/s13046-021-02239-4
- Yeo, N. C., Chavez, A., Lance-Byrne, A., Chan, Y., Menn, D., Milanova, D., Kuo, C.-C., Guo, X., Sharma, S., Tung, A. et al.** (2018). An enhanced CRISPR repressor for targeted mammalian gene regulation. *Nat. Methods* **15**, 611-616. doi:10.1038/s41592-018-0048-5
- Zhan, T., Rindtorff, N. and Boutros, M.** (2017). Wnt signaling in cancer. *Oncogene* **36**, 1461-1473. doi:10.1038/ncr.2016.304
- Zhang, N., Wei, P., Gong, A., Chiu, W.-T., Lee, H.-T., Colman, H., Huang, H., Xue, J., Liu, M., Wang, Y. et al.** (2011). FoxM1 promotes β -catenin nuclear localization and controls Wnt target-gene expression and glioma tumorigenesis. *Cancer Cell* **20**, 427-442. doi:10.1016/j.ccr.2011.08.016
- Zhao, T., Su, Z., Li, Y., Zhang, X. and You, Q.** (2020). Chitinase-3 like-protein-1 function and its role in diseases. *Signal Transduct. Target. Ther.* **5**, 201. doi:10.1038/s41392-020-00303-7
- Zheng, X., Lin, J., Wu, H., Mo, Z., Lian, Y., Wang, P., Hu, Z., Gao, Z., Peng, L. and Xie, C.** (2019). Forkhead box (FOX) G1 promotes hepatocellular carcinoma epithelial-Mesenchymal transition by activating Wnt signal through forming T-cell factor-4/ β -catenin/FOXG1 complex. *J. Exp. Clin. Cancer Res.* **38**, 475. doi:10.1186/s13046-019-1433-3
- Zimmerli, D., Borrelli, C., Jauregi-Miguel, A., Soderholm, S., Brutsch, S., Doumpas, N., Reichmuth, J., Murphy-Seiler, F., Aguet, M., Basler, K. et al.** (2020). TBX3 acts as tissue-specific component of the Wnt/ β -catenin transcriptional complex. *eLife* **9**, e58123. doi:10.7554/eLife.58123

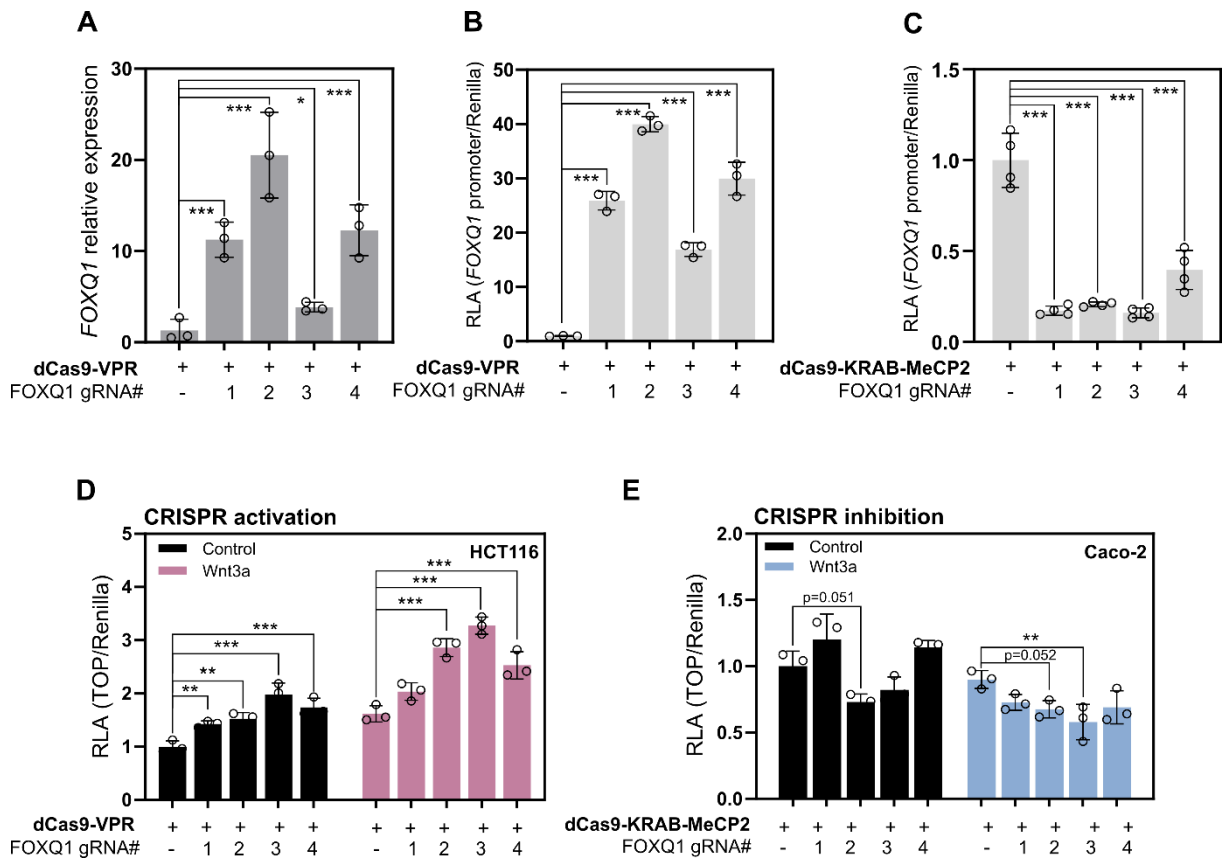


Fig. S1. FOXQ1 is a physiological activator of Wnt/ β -catenin signalling.

(A) *FOXQ1* qPCR in 293T cells. *FOXQ1* expression was significantly induced by a dCas9-VPR (CRISPR activation) construct guided to the *FOXQ1* promoter by four non-overlapping guide RNAs. Data are displayed as fold change compared to empty vector control and show biological triplicates. (B-C) Luciferase assay showing that CRISPR-mediated *FOXQ1* induction or inhibition activated (B) or repressed (C) a FOXQ1 promoter reporter construct, respectively. (D) TOPflash reporter assay showing that CRISPR-mediated induction of FOXQ1 activated Wnt/ β -catenin signalling in HCT116 cells. Data show one representative of $n = 2$ independent experiments with biological triplicates. (E) TOPflash reporter assay in Caco-2 cells. CRISPR-mediated inhibition of FOXQ1 decreased the reporter activity. Data represent an independent experiment with biological triplicates.

Data are displayed as mean \pm SD. Statistical significance was determined by ANOVA with Dunnett's post-hoc test (A-E), and defined as * $P < 0.05$, ** $P < 0.01$, *** $P < 0.001$.

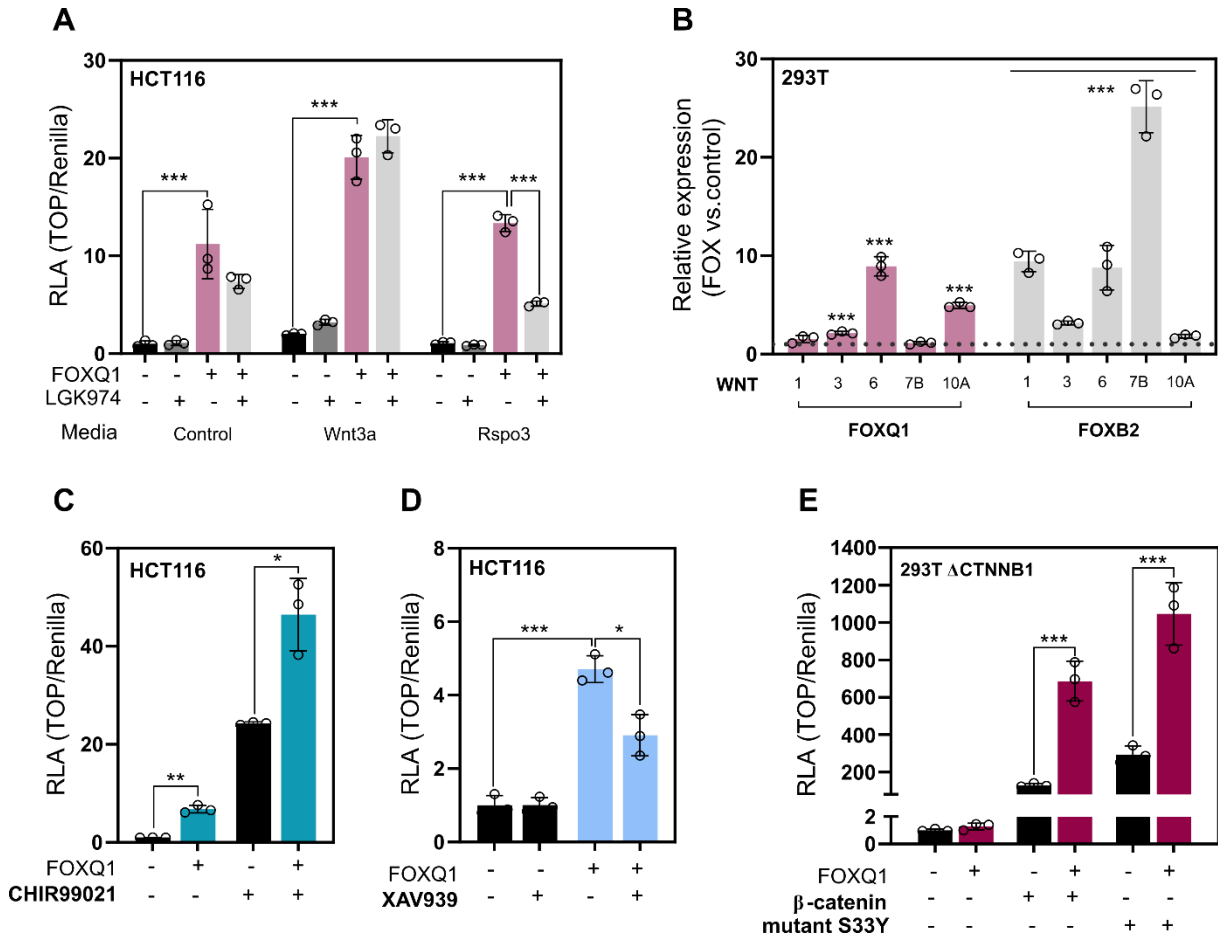


Fig. S2. FOXQ1 requires upstream pathway activation and β -catenin stabilisation to promote Wnt signalling.

(A) TOPflash assay in HCT116 cells in the presence of LGK974 (10 nM). Treatment with LGK974 attenuated FOXQ1-dependent Wnt activation, especially in the presence of exogenous R-spondin 3. Data show one representative of $n = 2$ independent experiments with biological triplicates. (B) qPCR of relevant Wnt ligands for comparison of FOXQ1 with FOXB2. Data are displayed as fold change compared to empty vector control and show biological triplicates. (C) TOPflash assay in HCT116 cells upon treatment with CHIR99021 (5 μ M). FOXQ1 strongly potentiated Wnt signalling in synergy with CHIR99021. Data show one representative of $n = 3$ independent experiments with biological triplicates. (D) TOPflash assay in HCT116 cells upon treatment with XAV939 (5 μ M). FOXQ1-dependent Wnt reporter activity was reduced upon β -catenin de-stabilization by XAV939. Data show one representative of $n = 3$ independent experiments with biological triplicates. (E) TOPflash assay in 293T cells lacking β -catenin. FOXQ1 did not activate the β -catenin/TCF reporter in the absence of β -catenin. However,

FOXQ1 synergized with exogenous wild-type and constitutively active β -catenin S33Y to activate Wnt signalling. Data show one experiment with biological triplicates. Data are displayed as mean \pm SD. Statistical significance was calculated by ANOVA with Tukey's post-hoc test (A, D, E) or Welch's t-test (B, C), and defined as * $P < 0.05$, ** $P < 0.01$, *** $P < 0.001$.

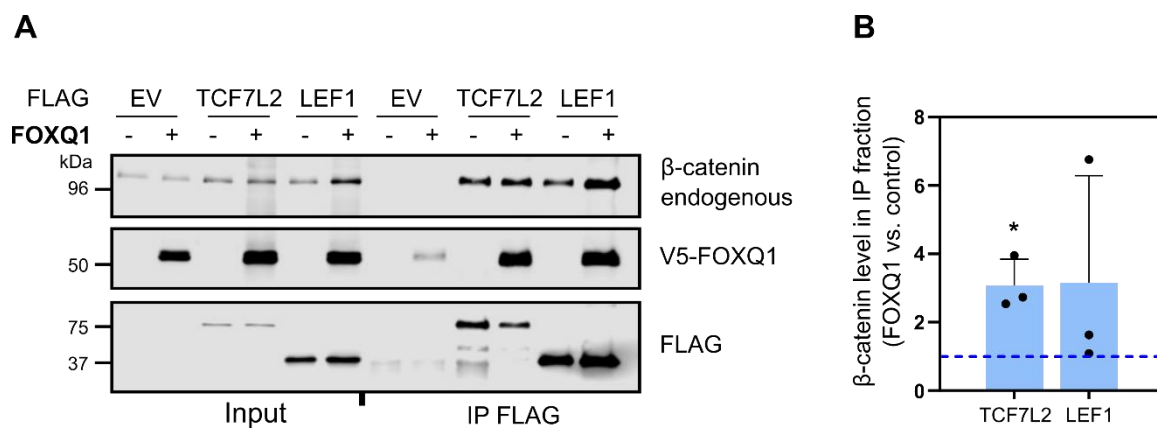


Fig. S3. FOXQ1 interacts with the Wnt transcriptional complex.

(A) Co-immunoprecipitation of Flag-tagged TCF7L2 and LEF1 from nuclear lysates of Wnt3a-treated 293T cells. Where indicated, cells were transfected with V5-FOXQ1. Following Flag pull-down, FOXQ1 and endogenous β -catenin were detected by immunoblotting. Data are representative of $n = 3$ independent experiments. (B) Relative abundance of β -catenin associated with TCF7L2 and LEF1 from the previous immunoprecipitation experiments. FOXQ1 significantly increased β -catenin association with TCF7L2.

Data are displayed as mean \pm SD. Statistical significance was calculated by Welch's t-test, and defined as $*P < 0.05$.

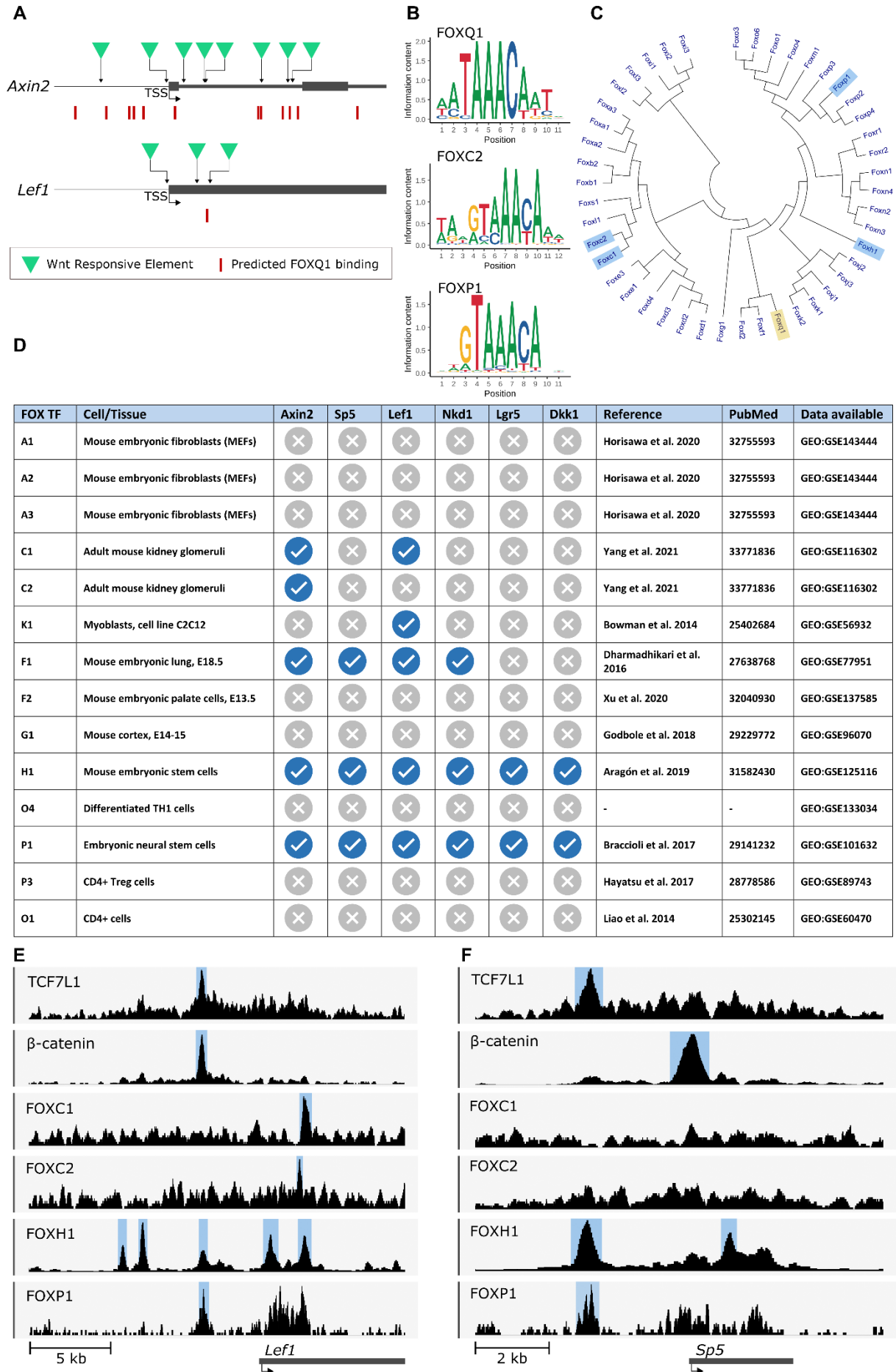


Fig. S4. FOX transcription factors bind at known Wnt target genes.

(A) Prediction of FOXQ1 binding sites at the mouse *Axin2* and *Lef1* loci, based on JASPAR 2022 binding profile data. Green triangles denote Wnt-responsive elements (WREs) required for TCF/LEF binding, as previously identified (Jho et al., 2002; Li et al., 2006). Red rectangles denote predicted FOXQ1 binding sites. (B) Sequence logo displaying the FOXQ1, FOXC2, FOXP1 consensus DNA-binding motif from the JASPAR database. (C) Phylogenetic tree of FOX transcription factors. Phylogenetic relationship between factors were determined based on their Forkhead box sequences. Highlighted in blue are FOX factors for which ChIP-seq genomic tracks are displayed. (D) Table of FOX transcription factors for which ChIP-seq data has been obtained, including references to dataset repositories and associated publications. Blue check symbol denotes the presence of a called ChIP-seq peak at the promoter region of the corresponding gene. Gray cross symbol denotes the absence of a binding event. Note: for FOXH1 and FOXP1, only sequence coverage data (i.e., no peak calling data) were found, and the presence of binding events at gene promoters was assessed by visual inspection of these signalling tracks. (E, F) Genomic tracks showing protein-DNA binding enrichment of TCF7L1, β -catenin, FOXC1, FOXC2, FOXH1 and FOXP1 at the *Lef1* and *Sp5* loci, obtained from publicly available ChIP-seq datasets.

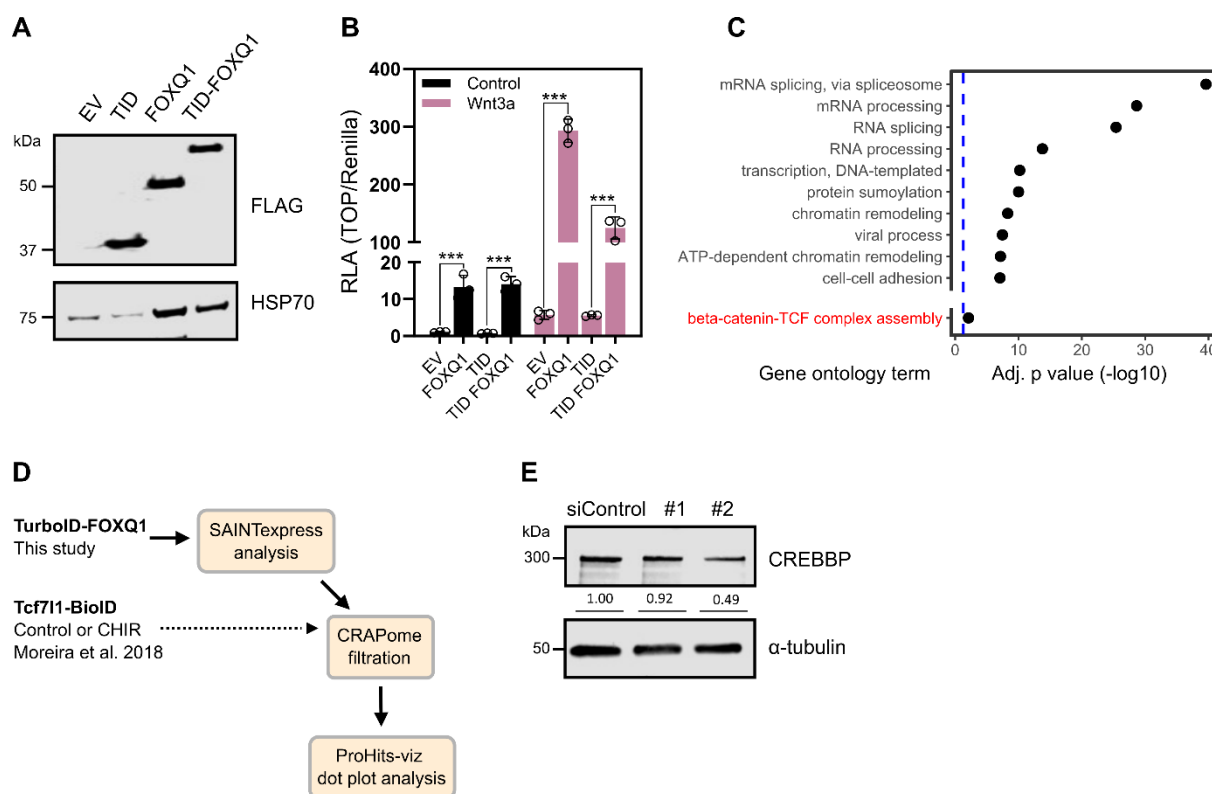
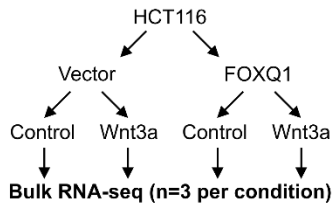


Fig. S5. FOXQ1 shares multiple co-factors with TCF/LEF.

(A) Immunoblot for protein expression of Flag-tagged TurboID-FOXQ1 fusion construct in 293T cells. TID, TurboID. (B) TOPflash assay for functional validation of the TID-FOXQ1 construct in 293T cells. The TID-FOXQ1 construct activated Wnt signalling similarly to wild-type FOXQ1. (C) Gene ontology (GO) analysis of the statistically significant FOXQ1 interactors identified using TurboID. Only the top 10 most significant GO terms are shown in addition to *beta-catenin-TCF complex assembly*. Full results can be found in Table S1. The dashed blue line indicates an adjusted p-value of 0.05. (D) Schematic representation of the workflow used for mass spectrometry data analysis. (E) Immunoblot analysis to confirm CREBBP silencing by RNA interference. Numbers of CREBBP protein quantification relative to the siRNA control are reported.

Data are displayed as mean \pm SD. Statistical significance was calculated by ANOVA with Tukey's post-hoc test (B) and defined as *** $P < 0.001$.

A



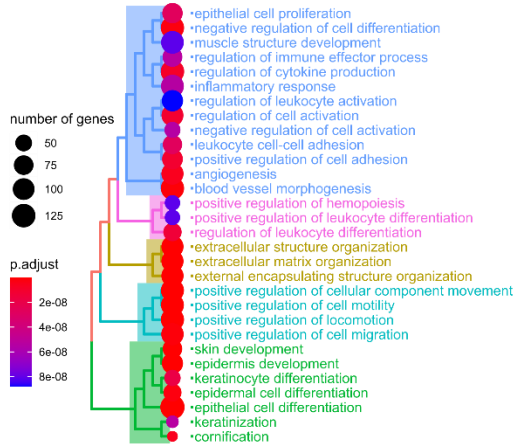
B

Differentially expressed genes (DEGs, FDR-adjusted p value < 0.05)

DEGs (up/down)	Condition			
	Vector-Control	Vector-Wnt3a	FOXQ1-Control	FOXQ1-Wnt3a
Vector-Control	-	166 (96/70)	4097 (1984/2113)	4924 (2150/2774)
Vector-Wnt3a		-	4950 (2395/2555)	4948 (2218/2730)
FOXQ1-Control			-	137 (74/63)
FOXQ1-Wnt3a				-

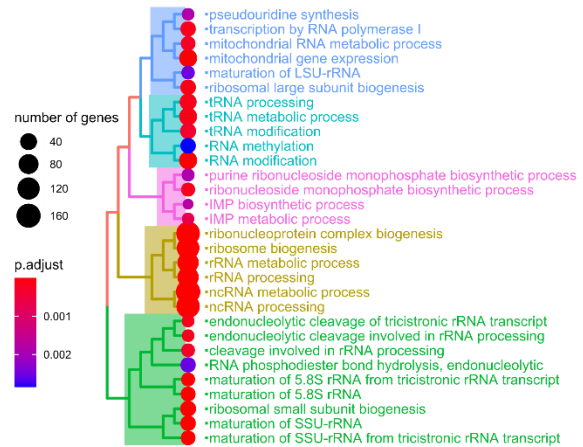
C

Genes upregulated by FOXQ1 (FDR < 0.05, log₂ FC > 0)

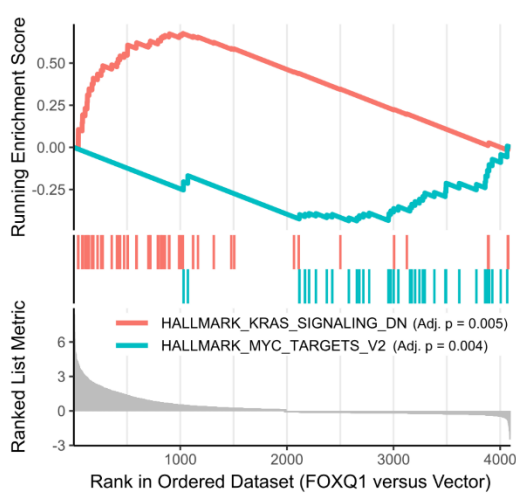


D

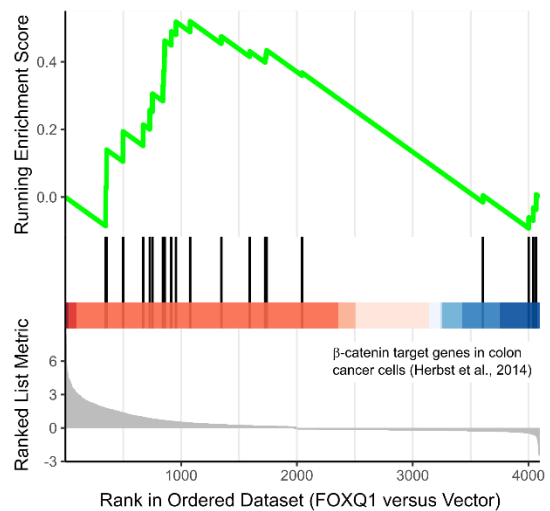
Genes downregulated by FOXQ1 (FDR < 0.05, log₂ FC < 0)



E



F



G

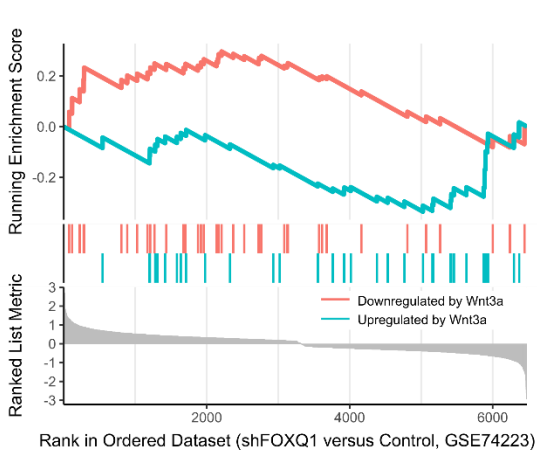


Fig. S6. FOXQ1 alters the transcriptome of colorectal cancer cells.

(A) Overview of the bulk RNA sequencing experiment performed in this study. (B) Summary of the number of differentially regulated protein-coding genes (DEGs) when comparing the different conditions. (C, D) Gene ontology analysis of FOXQ1-associated DEGs in untreated cells. Ontology terms were grouped using Ward's clustering algorithm. (E) Gene set enrichment analysis (GSEA) against all hallmark gene sets identified genes downregulated by KRAS and MYC target genes as the only significantly enriched sets in untreated FOXQ1-expressing cells. (F) GSEA using a curated list of β -catenin target genes indicated modest enrichment in untreated FOXQ1-expressing cells. (G) GSEA of 166 Wnt-regulated genes (see panel B) in DLD-1 cells transfected with FOXQ1 shRNA (GSE74223, n = 2 replicates per condition).

Fig. S7. Blot transparency

Fig. 3A

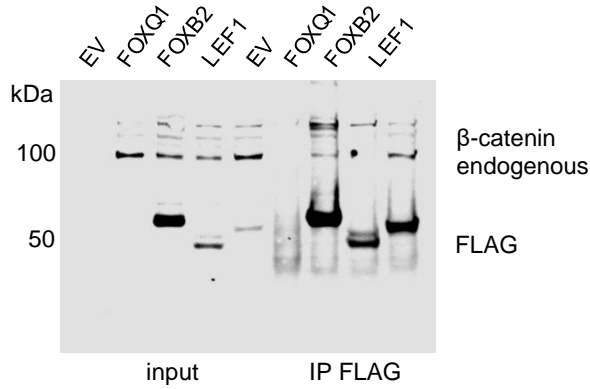


Fig. 3B

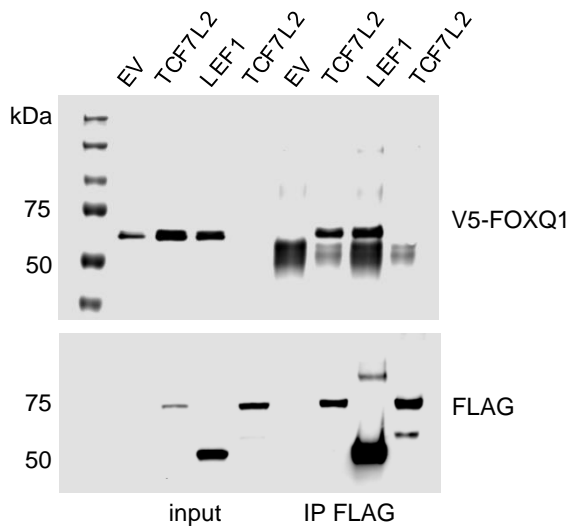


Fig. 3C

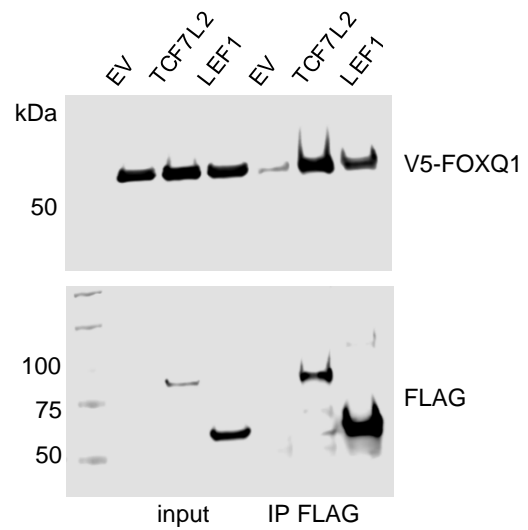


Fig. 3G

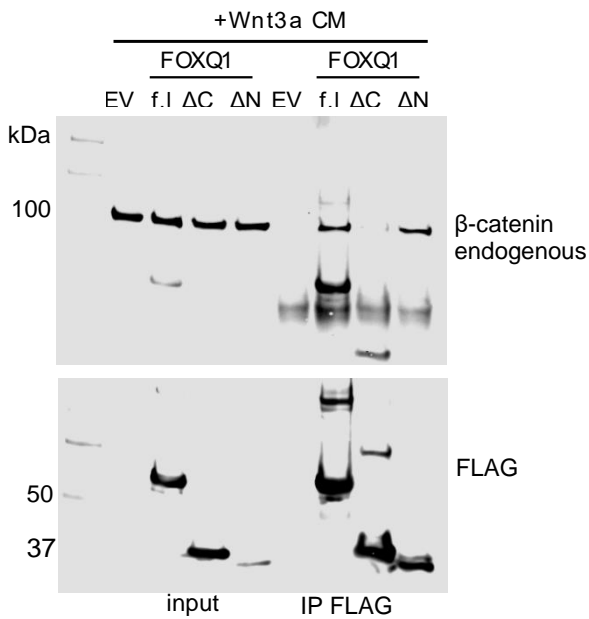


Fig. 3H

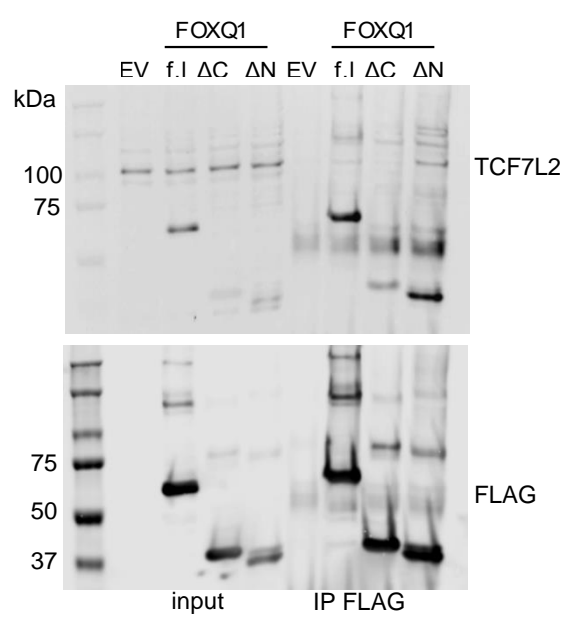


Fig. 5H

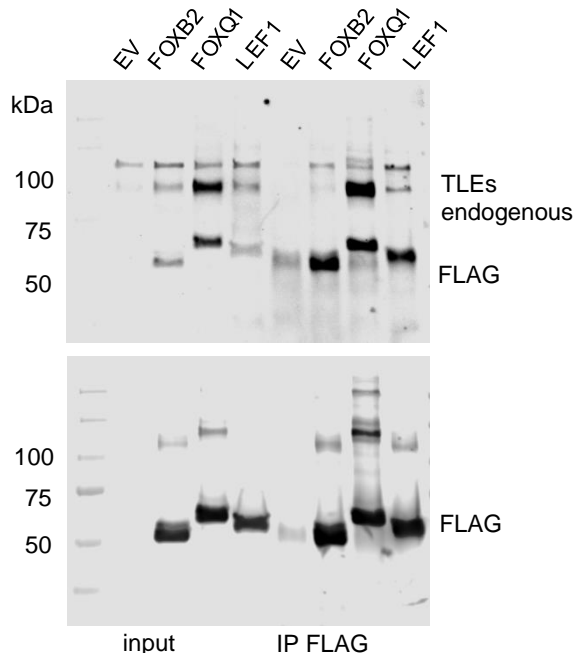


Fig. 5I

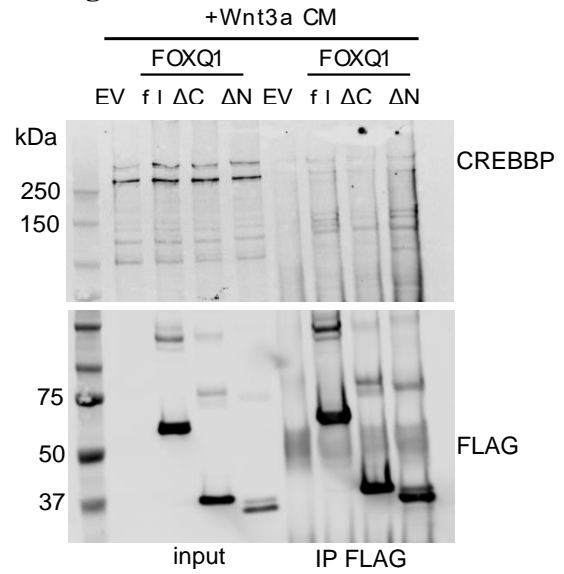


Fig. S3A

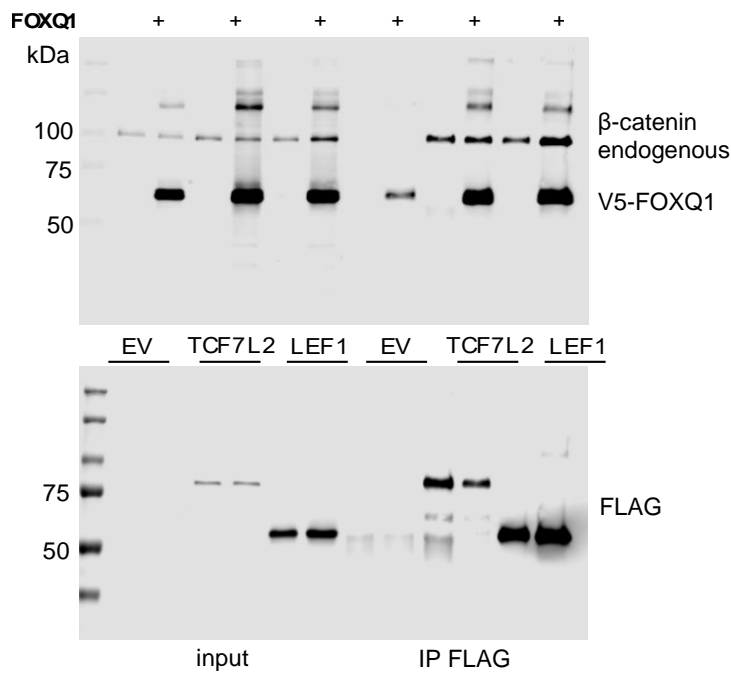


Fig. S5A

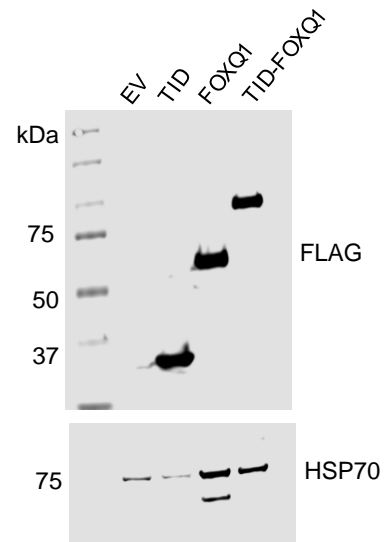


Fig. S5E

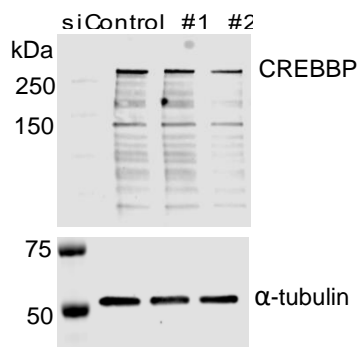


Table S1. Gene Ontology (GO) analysis of FOXQ1 TurboID experiments.

[Click here to download Table S1](#)

Table S2. SAINTexpress analysis of FOXQ1 TurboID experiments.

[Click here to download Table S2](#)

Table S3. SAINTexpress analysis of FOXQ1 + CHIR TurboID experiments.

[Click here to download Table S3](#)

Table S4. Ct values for the qPCR experiments included in the study.

[Click here to download Table S4](#)

References

Jho, E. H., Zhang, T., Domon, C., Joo, C. K., Freund, J. N. and Costantini, F. (2002). Wnt/beta-catenin/Tcf signaling induces the transcription of Axin2, a negative regulator of the signaling pathway. *Mol Cell Biol* **22**, 1172-83.

Li, T. W., Ting, J. H., Yokoyama, N. N., Bernstein, A., van de Wetering, M. and Waterman, M. L. (2006). Wnt activation and alternative promoter repression of LEF1 in colon cancer. *Mol Cell Biol* **26**, 5284-99.